International Journal of Scientific Research in Computer Science, Engineering and Information Technology
ISSN : 2456-3307 (www.ijsrcseit.com)
doi : https://doi.org/10.32628/IJSRCSEIT

Inverse Kinematic Analysis of 5-DOF and 7-DOF Redundant Manipulator using ANFIS

Mohit Kumar[1], B. S. Choudhary[2]

[1]M. Tech Student, Department of Mechanical Engineering, Millennium Institute of Technology, Bhopal, Madhya Pradesh, India

[2]Faculty, Department of Mechanical Engineering, Millennium Institute of Technology, Bhopal, Madhya Pradesh, India

ARTICLEINFO

Article History:

Accepted: 13 March 2023
Published: 18 March 2023

Publication Issue
Volume 10, Issue 2
March-April-2023

Page Number
97-127

ABSTRACT

Robots are one of the prominent aspects of current technological advancements. Current research study focuses on conducting Inverse Kinematic Analysis of 5-DOF & 7-DOF Redundant Manipulator using ANFIS. ANFIS stands for Adaptive Neuro-fuzzy Inference system. In this study ANFIS modelling has been performed to solve complex, nonlinear and discontinuous kinematics equation for a complex robot manipulator. It is also desired to find an ANFIS approach that provides a general frame work for combination of NN and fuzzy logic.The difference in joint angle deduced and predicted with ANFIS model for a 5-DOF and 7-DOF Redundant manipulator clearly depicts that the proposed method results with an acceptable error. Predicted (training data) values range from (-0.01 to 0.01) for both 5-DOF & 7- DOF and finding values (testing data) are range from (-0.03 to 0.03) it means the value decrease is about 0.02. The methods used for deriving the inverse kinematics model for these manipulators could be applied to other types of robotic arms, such as the EduBots developed by the Robotica Ltd, Pioneer 2 robotic arm (P2Arm), 5-DOF Lynx 6 Educational Robot arm. It can be concluded that the solution developed in this paper will make the PArm more useful in application with unpredicted trajectory movement in unknown environment.

Keywords :- Robots, Redundant Manipulator, ANFIS, inverse kinematics

I. INTRODUCTION

Word robot was coined by a Czech novelist Karel Capek in 1920. The term robot derives from the Czech word robot, meaning forced work or compulsory service. A robot is reprogrammable, multifunctional manipulator designed to move material, parts,

tools, or specialized devices through various programmed motions for the performance of a variety of tasks [1]. A simpler version it can be define as, an automatic device that performs functions normally ascribed to humans or a machine in the form of a human.

1.2. HISTORY OF ROBOTICS

The first industrial robot named UNIMATE; it is the first programmable robot designed by George Devol in1954, who coined the term Universal Automation. The first UNIMATE was installed at a General Motors plant to work with heated die-casting machines.

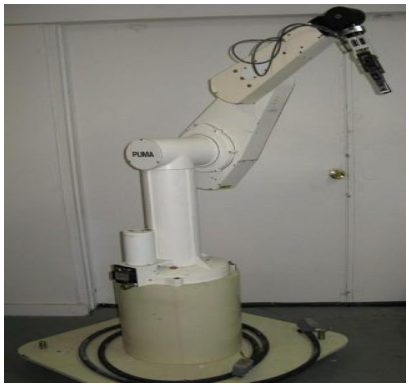

FIGURE 1.1 THE FIRST INDUSTRIAL ROBOT: UNIMATE

In 1978, the Puma (Programmable Universal Machine for Assembly) robot is developed by Victor Scheinman at pioneering robot company Unimation with a General Motors design support. These robots are widely used in various organisations such as Nokia corporation, NASA, Robotics and Welding organization.

Then the robot industries enters a phase of rapid growth to till date, as various type of robot are being developed with various new technology, which are being used in various industries for various work. Few of these milestones in the history of robotics are given below.

1947 — The first served electric powered teleoperator is developed.

1948 — A teleoperator is developed incorporating force feedback.

1949 — Research on numerically controlled milling machine is initiated.

1954 — George Devol designs the first programmable robot.

1956 — Joseph Engel Berger, a Columbia University physics student, buys the rights to Devol's robot and founds the Unimation Company.

1961 — The first Unimate robot is installed in a Trenton, New Jersey plant of General

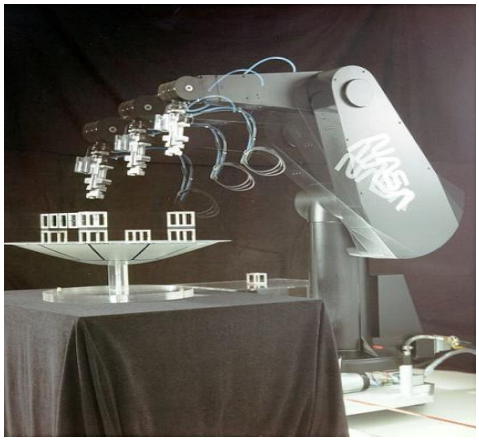

Motors to tend an die casting machine.

FIGURE 1.2PUMA ROBOTIC ARM

1961 — The first robot incorporating force feedback is developed.

1963 — The first robot vision system is developed.

1971 — The Stanford Arm is developed at Stanford University.

1973 — The first robot programming language (WAVE) is developed at Stanford.

1974 — Cincinnati Milacron introduced the T3 robot with computer control.

1975 — Unimation Inc. registers its first financial profit.

1976 — The Remote Center Compliance (RCC) device for part insertion in assembly isdeveloped at Draper Labs in Boston.

1976 — Robot arms are used on the Viking I and II space probes and land on Mars.

1978 — Unimation introduces the PUMA robot, based on designs from a General Motors study.

1.3. LAWS OF ROBOTICS

Asimovproposed three "Laws of Robotics", and later added a 'Zeroth law'.

Zeroth Law: A robot may not injure humanity, or, through inaction, allow humanity to come to harm.

First Law: A robot may not injure a human being, or, through inaction, allow a human being to come to harm, unless this would violate a higher order law.

Second Law: A robot must obey orders given it by human beings, expect where such orders would conflict with a higher order law.

Third Law: A robot must protect its own existence as long as such protection does not conflict with a higher order law.

1.4. COMPONENTS AND STRUCTURE OF ROBOTS

The basic components of an industrial robot are:

- The manipulator
- The End-Effector (Which is a part of the manipulator)
- The Power supply
- The controller

Robot Manipulators are composed of links connected by joints into a kinematic chain.

Joints are typically rotary (revolute) or linear (prismatic). A revolute joint rotates about a motion axis and a prismatic joint slide along a motion axis. It can also be defined as a prismatic joint is a joint, where the pair of links makes a translational displacement along a fixed axis. In other words, one link slides on the other along a straight line. Therefore, it is also called a sliding joint. A revolute joint is a joint, where a pair of links rotates about a fixed axis. This type of joint is often referred to as a hinge, articulated, or rotational joint.

Prismatic

Revolute

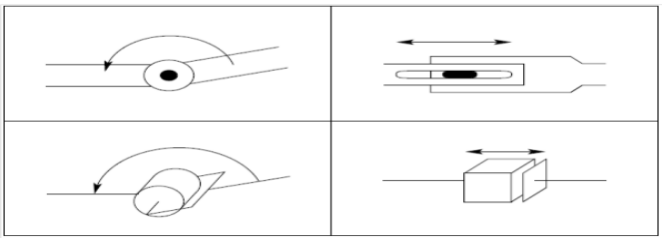

FIGURE 1.3. SYMBOLIC REPRESENTATION OF ROBOT JOINTS.

The end-effector which is a gripper tool, a special device, or fixture attached to the robot's arm, actually performs the work.

Power supply provides and regulates the energy that is converted to motion by the robot actuator, and it may be electric, pneumatic, or hydraulic.

The controller initiates, terminates, and coordinates the motion of sequences of a robot. Also, it accepts the necessary inputs to the robot and provides the outputs to interface with the outside world. In other words, the controller processes the sensory information and computes the control commands for the actuator to carry out specified tasks.

1.5. REDUNDANT MANIPULATOR

A manipulator is required have a minimum of six degree of freedom if it needs to acquire any random position and orientation in its operational space or work space. Assuming one joint is required for each degree of freedom, such a manipulator needs to be composed of minimum of six joints. Usually in standard practice three degree of freedom is implemented in the robotic arm so it can acquire the desired position in its work space. The arm is then fitted with a wrist composed of three joints to acquire the desired orientation. Such a manipulator is called non-redundant. Though non-redundant manipulators are kinematically simple to design and solve, but the non-redundancy leads to two

fundamental problems: singularity and inability to avoid obstacles. The singularities of the robot manipulator are present both in the arm and the wrist and can occur anywhere inside the workspace of the manipulator. While passing through these singularities, the manipulator can effectively lose certain degree of freedom, resulting in uncontrollability along those directions. The obstacle avoidance is another desirable characteristic to effectively plan the motion trajectories, especially for manipulators designed to perform demanding tasks in constricted environment. The above two problems can be solved by adding an additional degree of freedom to the manipulator This additional degree of freedom can be added to the joints, which effectively become singular in certain positions like shoulder, elbow, or wrist and hence help to overcome the singularities or obstacles avoidance. So, a redundant manipulator should possess at least one degree-of-freedom (DOF) more than the number required for the general free positioning. The Redundant can also be define as, when a manipulator can reach a specified position with

more than one configuration of the linkages, the manipulator is said to be redundant. From a general point of view, any robotic system in which the way of achieving a given task is not unique may be called redundant.

A redundant manipulator offers several potential advantages over a non-redundant manipulator. The extra DOF that require for the free positioning of manipulator can be used to move around or between obstacles and thereby to manipulate in situations that otherwise would be inaccessible. Due to the redundancy the manipulators become flexible, compliant, extremely dexterous and capable of dynamic adaptive, in unstructured environment.

1.6. DEGREE OF FREEDOM (DOF)

The number of joints determines the degrees-of-freedom (DOF) of the manipulator. Typically, a manipulator should possess at least six independent DOF: three for positioning and three for orientation. With fewer than six DOF the arm cannot reach every point in its work environment with arbitrary orientation. Certain applications such as reaching around or behind obstacles require more than six DOF. The difficulty of controlling a manipulator increases rapidly with the number of links. A manipulator having more than six links is referred to as a kinematically redundant manipulator.

1.7. MOTIVATIONS

The motivation for this thesis is to obtain the inverse kinematic solutions of redundant manipulator such as 5-DOF Redundant manipulator and 7-DOF Redundant manipulator. As the inverse kinematic equation of these types of manipulators contain non-linear equations, time varying equations and transcendental functions. Due to the complexity in solving this type of equation by geometric, iterative or algebraic method is very difficult and time consuming. It is very important to solve the inverse kinematics solution for this type of redundant manipulator to know the exact operational space and to avoid the obstacles. So various researcher had applied various methods for solving the kinematic equation. L. Sciavicco et al. used inverse Jacobian, pseudo inverse Jacobian or Jacobian transpose and solve the IK problem of 7-DOF redundant manipulator iteratively. But the main drawback of this method is, these are slow and suffer from singularity issue. Shimizu et al. proposed an IK solution for the PA 10-7C 7-DOF manipulator and considered arm angle as redundancy parameter. In his study, a detailed analysis of the variation of the joint angle with the arm angle parameter is considered, which is then utilizes for redundancy resolution. However, link offset was not considered in his work. Some

authors also applied ANN, due to its adapting and learning nature. Although ANN are very efficient in adopting and learning but they have the negative attribute of 'black box'. To overcome this drawback, various author adopted neuro fuzzy method like ANFIS (Adaptive Neuro-fuzzy Inference system). This can be justified as ANFIS combines the advantage of ANN and fuzzy logic technique without having any of their disadvantage. The neuro fuzzy system is must widely studied hybrid system now a days, as due to the advantages of two very important modelling technique i.e.,NN and Fuzzy logic.So, the goal of this thesis is to predict the inverse kinematics solution for the redundant manipulator using ANFIS. As a result, suitable posture and the trajectories for the manipulator can be planned for execution of different work in various fields.

1.8. OBJECTIVES OF THE THESIS

The objective of this thesis is to solve the inverse kinematics equations of the redundant manipulator. The inverse kinematics equations of this type of manipulator are highly unpredictable as this equation are highly non-linear and contains transcendental function. The complexity in solving this equation increases due to increase in higher DOF. So various authors had used neuro-fuzzy method (ANFIS) to solve the non-linear and complex equations arise in different field. ANFIS was adopted by different researcher in their work, for mathematical modelling of the data, as it has high range of potential for solving the complex and nonlinear equations arise in different field like in marketing, manufacturing industries, civil engineering etc. Li ke et al. applied ANFIS to solve the forecast problem of microwave effect by adopting microwave parameters and its threshold as variable. Then they develop an ANFIS model to study its forecasting ability. By comparing the output of ANFIS with training and testing data, they concluded with good forecasting ability, small error and low data requirement are found with ANFIS. Srinivasan et al. applied ANFIS based on PD plus I controller to the dynamic model of 6-DOF robot manipulator (PUMA Robot). Numerical simulation using the dynamic model of 6-DOF robot arm shows the effectiveness of the approach in trajectory tracking problems. After the successfully implementation of ANFIS in various field for solving the non-linear equations, it is concluded that ANFIS is a best technique can be used for solving the non-linear equation arises in the inverse kinematic equation in robotics.

The architecture and learning procedure underlying ANFIS (adaptive-network-based fuzzy inference system) is presented, which is a fuzzy inference system implemented in the framework of adaptive networks. By using a hybrid learning procedure, the proposed ANFIS can construct an input-output mapping based on both human knowledge (in the form of fuzzy if-then rules) and stipulated input-output data pairs. In the simulation, the ANFIS architecture is employed to model nonlinear functions, identify nonlinear components on-line in a control system, and predict a chaotic time series, all yielding remarkable results. Comparisons with artificial neural networks and earlier work on fuzzy modeling are listed and discussed.

Fuzzy inference system (FIS) and artificial neuro-fuzzy inference system (ANFIS) as two powerful tools for iterative optimization of complex energy systems as well as real-time optimization of energy systems were presented in this chapter. The complete methodologies of two methods were discussed in detail, and these tools were examined on two case studies, including the CGAM problem and a fossil-fueled steam power plant. It was proved that these tools have fast calculation speed to find an optimal solution that makes them suitable tools for real-time

optimization of the energy system and optimization of complex energy systems.

It was discussed that the requirement to complex fuzzy data (including fuzzy rules and membership functions) is a severe barrier to the usage of the FIS in real cases.

Nevertheless, the ANFIS tool was presented as a favorite tool for the generation of the required fuzzy data that are acquired by the FIS in an automatic process. The robustness and speed of the ANFIS were examined on two case studies, and its superior calculation speed and accuracy were proved compared to conventional optimization methods such as the genetic algorithm (GA). It was observed that the ANFIS could generate all required fuzzy data that were already employed by the FIS. Still, there is something like the type of membership functions and the number of nodes at the input/output layers of the ANFIS network that must be specified in a trial-and-error process. In future research, the approach to find an optimal structure of the ANFIS network might be studied. Based on this chapter, the ANFIS method is recommended as the foremost optimization tool for real-time optimization of energy systems as well as optimization of complex energy systems and everywhere that high-speed optimization tool is required. This approach would be examined on more complex problems in future studies.

1.9 APPLICATIONS AND BENEFITS OF FIS

Fuzzy inference systems have been applied to several interesting and practical tasks, such as for the selection of the architecture, technology, and characteristics of a demotic system; cotton thread strength modeling, human disease diagnosis (as diabetes, cardiac, and tropical diseases), teacher performance evaluation, human internet consultant, water quality assessment, estimation of productivity in construction work, improved oil recovery, integral oil exploration, evaluation of intellectual capital performance, processing of loans to small companies, qualification of clients for bank loans, strategic investments, prediction of some quality characteristics of concentrated grape juice, among others.

Among the main benefits of FIS are reducing the cost of application development, reducing execution costs, reducing maintenance costs, among others. These benefits are because fuzzy inference systems are more compact (require fewer rules), encode high-level knowledge, and even in the designer's native language, they are less prone to errors, handle vague, uncertain, and imprecise information, and they are much easier to maintain. Finally, the Sugeno FIS are especially relevant, because they support the modeling and building of hybrid systems, such as adaptive neuro-fuzzy inference system (ANFIS) and adaptive neuro-fuzzy system with linguistic hedges. On the other hand, the Mamdani FIS is taken as base for the hybrid system for classification NEFCLASS.

1.10 ADAPTIVE NETWORK-BASED FUZZY INFERENCE SYSTEM

Fuzzy logic proposed by Zadeh in 1965 is a popular computing framework that consists of fuzzy set theory, fuzzy if-then rules, and fuzzy reasoning. By integrating the fuzzy systems with the ANN models, an effective tool is obtained that takes advantage of the learning characteristics of the ANN models and has a performance equal to an inference fuzzy model as well. The neuro-fuzzy system corresponds to a fuzzy model of Takagi–Sugeno, wherein the weights of the ANN model are similar to the parameters of the fuzzy system. This structure that is called ANFIS was developed by Jang in 1995. ANFIS, which is a hybrid model, composed of a fuzzy and artificial neural network, aims to determine the behavior of imprecisely complex dynamic systems and to deal with engineering problems.

ANFIS includes an adaptive ANN and a fuzzy inference system and uses a hybrid-learning rule

merging gradient descent, back propagation, and a least-squares algorithm to determine a set of parameters. ANFIS can be considered as a responsive mathematical structure that can estimate a large class of complex nonlinear systems to a desired degree of precision at the computational level. The ANFIS structure consists of five layers, namely, fuzzy layer, product layer, normalized layer, de-fuzzy layer, and total output layer.

Layer 1: In this layer, every node is an adaptive node. Membership functions such as generalized bell membership function and Gaussian membership function are used as node function.

Layer 2: In this layer, each node output shows the firing strength of a rule.

Layer 3: Every node represents the normalized firing strength of each rule.

Layer 4: In this layer, every node is an adaptive node with a node function indicating the contribution of the rules toward the overall output. Parameters in this layer will be referred to as consequent parameters.

Layer 5: There is a single node that calculates the sum of all the rules' outputs.

In this study, different ANFIS models using seven input parameters are developed for estimating GSR by using training data of the eight cities. Then, results of these ANFIS models are compared with measured data for testing years.

II. LITRTURE REVIEW

Calderon et al. [2022] proposed a hybrid approach to inverse kinematics and control and a resolve motion rate control method are experimented to evaluate their performances in terms of accuracy and time response in trajectory tracking.

Xu et al. [2021] proposed an analytical solution for a 5-DOF manipulator to follow a given trajectory while keeping the orientation of one axis in the end-effector frame by considering the singular position problem.

Gan et al. [2020] derived a complete analytical inverse kinematics (IK) model, which is able to control the P2Arm to any given position and orientation, in its reachable space, so that the P2Arm gripper mounted on a mobile robot can be controlled to move to any reachable position in an unknown environment. Utilization of artificial neural networks (ANN) and fuzzy logic for solving the inverse kinematics equation of various robotic arms is also considered by researchers.

Hasan and Assadi [2019] adopted an application of ANN to the solution of the IK problem for serial robot manipulators. In his study, two networks were trained and compared to examine the effect of the Jacobian matrix to the efficiency of the inverse kinematics solution.

Sciavicco et.al. [2019] used inverse Jacobian, pseudo inverse Jacobian or Jacobian transpose and solve the IK problem of 7-DOF redundant manipulator iteratively. But the main drawback of this method is, these are slow and suffer from singularity issue.

Shimizu et.al. [2017] proposed an IK solution for the PA 10-7C 7-DOF manipulator and considered arm angle as redundancy parameter. In his study, a detailed analysis of the variation of the joint angle with the arm angle parameter is considered, which is then utilizes for redundancy resolution. However, link offset was not considered in his work. An analytical solution for IK of a redundant 7-DOF manipulator with link offset was carried out

G.K Singh and J. Claassens [2016]. They have considered a 7-DOF Barrett whole arm manipulator with link offset and concluded that the possibility of in-elbow and out-elbow poses of a given end-effector pose arise due to the presence of link offset. They also presented a geometric method for computing the joint variable for any geometric pose.

Dahm and Jublin [2016] used angle parameter as redundancy and derived a closed-form inverse solution of 7-DOF manipulator. They also analysed the limitation of the parameter caused by a joint limit based on a geometric construction. The analysis has

its own drawback as priority is being given to one of the wrist joint limit. Based on the closed-form inverse solution and using angle parameters by Dahm and Joublin in his work,

Mandel et.al. [2015] used ANN with back propagation as learning algorithm to model EDM process. They concluded that by considering different input parameters such as roughness, material removal rate (MRR), and Tool wear rate (TWR) are found to be efficient for predicting the response parameters.

Panda and Bhoi [2014], predicted MRR of D2 grads steel by developing an artificial feed forward NN model based on Levenberg-Marquardt back propagation technique and logistic sigmoid activation function. The model performs faster and provides more accurate result for predicting MRR.

Goa et.al. [2013] considered different algorithm like L-M algorithm, resilient algorithm, Gausi-Newton algorithm to established different model for machining process. After several training of models and comparing the generalization performance they conclude that L-M algorithm provides faster and more accurate result. Despite of the NN approach by different authors as discussed above, some authors have also adopted neuro fuzzy (NF) method for solving non-linear and complex equation. Although ANN are very efficient in adopting and learning but they have the negative attribute of 'black box'. To overcome this drawback, various author adopted neuro fuzzy method like ANFIS. This can be justified as ANFIS combines the advantage of ANN and fuzzy logic technique without having any of their disadvantage.

Malki et.al. [2012]adopted adaptive neuro fuzzy relationships to model the UH-60A Black Hawk pilot floor vertical vibration. They have considered 200 data of UH-60A helicopter flight envelop for training and testing purpose. They conducted the study in two parts i.e. the first part involves level flight conditions and the second part involves the entire (200 points) database including maneuver condition. They concluded from their study that neuro fuzzy model can successfully predict the pilot vibration.

LI ke et.al. [2011] applied ANFIS to solve the forecast problem of microwave effect by adopting microwave parameters and its threshold as variable. Then they develop an ANFIS model to study its forecasting ability. By comparing the output of ANFIS with training and testing data, they concluded with good forecasting ability, small error and low data requirement are found with ANFIS.

Srinivasan et.al. [2010] applied ANFIS based on PD plus I controller to the dynamic model of 6-DOF robot manipulator (PUMA Robot). Numerical simulation using the dynamic model of 6-DOF robot arm shows the effectiveness of the approach in trajectory tracking problems. Comparative evaluation with respect to PID, fuzzy PD+I control are presented to validate the controller design. They concluded that a satisfactory tracking precision could be achieved using ANFIS based PD+I controller combination than fuzzy PD+I only or conventional PID only.

Roohollah Noori et.al [2009], predicted daily carbon monoxide (CO) concentration in the atmosphere of Tehran by means of ANN and ANFIS models. In this study they used Forward selection (FS) and Gamma test (GT) methods, for selecting input variables for developing hybrid models with ANN and ANFIS. They concluded that Input selection improves prediction capability of both ANN and ANFIS models and it not only reduces the output error but reduces the time of calculation due to less input variable.

U. Yüzgeç et.al., [2008], investigates different modelling approaches and compares for drying of baker's yeast in a fluidized bed dryer based on ANN and ANFIS. In this work they investigate four modelling concepts: modelling based on the mass and energy balance, modelling based on diffusion mechanism in the granule, modelling based on recurrent ANN and modelling based on ANFIS, to predict the dry matter of product, product temperature and product quality.

Mahmut Bilgehan [2007], carried out the buckling analysis of slender prismatic columns with a single non-propagating open edge crack subjected to axial loads, using ANFIS and ANN model. The main feature of his work is to study the feasibility of using ANFIS and NN for predicting the critical buckling load of fixed-free, pinned-pinned, fixed-pinned and fixed-fixed supported, axially loaded compression rods. After the comparative study made using NN and NF technique, he concluded that the proposed ANFIS architecture with Gaussian membership function is found to perform better than the multilayer feed forward ANN learning by back propagation algorithm.

Mahmut Bilgehan [2006], again considered the same model of NN and NF as used for analysis of slender prismatic columns, and had successfully applied it for the evaluation of relationships between concrete compressive strength and ultrasonic pulse velocity (UPV) values using experiment data obtained from many cores taken from different reinforced concrete structure having different ages and unknown ratio of concrete mixture. He carried out a comparative study of NN and NF technique on the basis of statistical measure to evaluate the performance of the model used. Then by comparing the result, he found that the proposed ANFIS architecture performed better than the multilayer feed-forward ANN model.

Jang [2004] reported that the ANFIS can be employed to model nonlinear functions, identify nonlinear components on-line in a control system, and predict a chaotic time series. It is a hybrid neuro-fuzzy technique that brings learning capabilities of neural networks to fuzzy inference systems. The learning algorithm tunes the membership functions of a Mamdani or Sugeno-type Fuzzy Inference System using the training input-output data.

Sadjadian et al., [2003]. Due to its high interpretability and computational efficiency and built-in optimal and adaptive techniques, ANFIS is widely used in pattern recognition, robotics, nonlinear regression, nonlinear system identification and adaptive system processing and also it can be used to predict the inverse kinematics solution. It is to be noted that ANFIS is suitable for solving complex, nonlinear mathematical equation for control of higher DOF robot manipulators.

III. PROBLEM IDENTIFICATION

- The data predicted with ANFIS for 5-DOF and 7-DOF Redundant manipulator, in this work clearly depicts that the proposed method results in an acceptable error.
- The forecast problem of microwave effect by adopting microwave parameters and its threshold as variable.
- The complexity of the solutions increases with higher DOF due to robot geometry, non-linear equations and singularity problems.

IV. RESEARCH OBJECTIVE

Main objectives of present work have been laid down here,

- In this study we have to find out the inverse kinematics solution using ANFIS for a 5-DOF and 7-DOF redundant manipulator is presented.
- In this study have to done ANFIS modelling to solve complex, nonlinear and discontinuous kinematics equation complex robot manipulator.
- Find an ANFIS approach that provides a general frame work for combination of NN and fuzzy logic.

4.1 FORWARD KINEMATICS AND INVERSE KINEMATICS

In this section of the thesis the forward kinematics and the inverse kinematics of the 5-DOF and 7- DOF redundant manipulator is discussed. The Denavit-Hartenberg (D-H)notation for these two manipulators is discussed with steps used for deriving the

forwardkinematics is presented. Then this chapter is concluded with the solution of inversekinematics for the 5-DOF redundant manipulator is given.

The forward kinematics is concerned with the relationship between the individual jointsof the robot manipulator and the position (x, y, and z) and orientation (ϕ) of the end-effector. stated more formally, the forward kinematics is to determine the position and orientationof the end-effector, given the values for the joint variables ($\theta_i, a_i, d_i, \alpha_i$)of the robot. Thejoint variables are the angles between the links in the case of revolute or rotational joints, andthe link extension in the case of prismatic or sliding joints. The forward kinematics is to becontrasted with the inverse kinematics, which will be studied in the next section of thischapter, and which is concerned with determining values for the joint variables that achieve adesired position and orientation for the end-effector of the robot. The above mention theory isexplained diagrammatically in figure 4.1

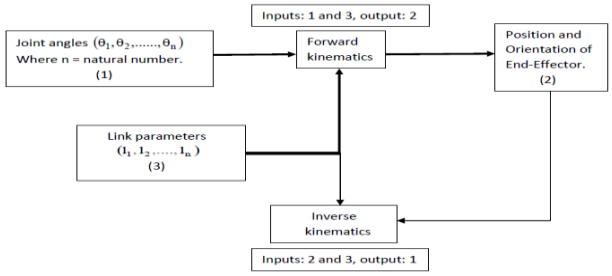

FIGURE 4.1 FORWARD AND INVERSE KINEMATICS SCHEME

4.2. DENAVIT-HARTENBERG NOTATION (D-H NOTATION)

A Robot manipulator with n joints (from 1 to n) will have n+1 links (from 0 to n,starting from base), since each joint connect to two links. By this convention, joint i connectlink i-1to link i. It is considered that the location of the joint to be fixed with respect to link i-1. Each link of the robot manipulator is considered to be rigidly attached to a coordinateframe for performing the kinematics analysis. In particular, link i is attached to $o_i\ x_i\ y_i\ z_i$. Itimplies that whenever the robot executes motion, the coordinate of each point on the link iare constant when expressed in the i^{th} coordinate frame. Furthermore, when joint i actuate,link i and its attached frame $o_i\ x_i\ y_i\ z_i$, and experience a resulting motion. The frame $o_i\ x_i\ y_i\ z_i$ is ainertial frame as it attached to the robot base.

Now suppose, A_i is the homogeneous transformation matrix that expresses the position andorientation of $o_i\ x_i\ y_i\ z_i$with respect to $o_{i-1}\ x_{i-1}\ y_{i-1}\ z_{i-1}$where matrix A_i is not constant butvaries as the configuration of the robot changes. Again, the homogeneous transformationmatrix that expresses the position and orientation of $o_j\ x_j\ y_j\ z_j$with respect to $o_i\ x_i\ y_i\ z_i$is called,by convention, a global transformation matrix and denoted by T_j.

Where,

$$T_j^i = A_{i+1}A_{i+2}\ldots A_{j-1}A_j \text{ if } i < j$$

$$T_j^i = I \text{ if } i = j$$

$$T_j^i = \left(T_i^j\right)^{-1} \text{ if } j > i$$

As the links are rigidly attached to the corresponding frame, it concludes that the position of any point on the end-effector, when expressed in the frame n, is a constant independent of the configuration of the robot. Hence the transformation matrix gives the position and orientation of the end-effector with respect to the inertial frame. So, D-H notation of the joint is introduced with some convention to solve this matrix. The convention and steps for D-H notation is represented as follows.

The following steps based on D-H notation are used for deriving the forward kinematics,

Step 1: Joint axes $Z_0 \ldots\ldots Z_{n-1}$is located and labelled.

Step 2: Base frame is assigned. Set the origin anywhere on the Z_0 –axis. The X_0 and Y_0 axes are chosen conveniently to form a right-hand frame.

Step 3: The origin Oi is located, where the common normal to Z_i and Z_{i-1} intersects at Z_i. If$Z_i$intersects Z_{i-1},

located at this intersection. If Z_i and Z_{i-1} are parallel, locate $O_i$inany convenient position along Z_i.

Step 4: X_i is considered along the common normal between Z_{i-1} and Z_i through O_i, or inthedirection normal to the Z_{i-1} - Z_i plane if Z_{i-1} and Z_i intersect.

Step 5:Y_i is established to complete a right-hand frame.

Step 6: The end-effector frame is assigned as $O_nX_nY_nZ_n$. Assuming thenth joint is revolute,set Z_n= a along the direction Z_{n-1}. The origin on is taken conveniently along $Z_n$direction, preferably at the centre of the gripper or at the tip of any tool that themanipulator may be carrying.

Step 7: All the link parameters$\theta_i, a_i, d_i, \alpha_i$are tabulated.

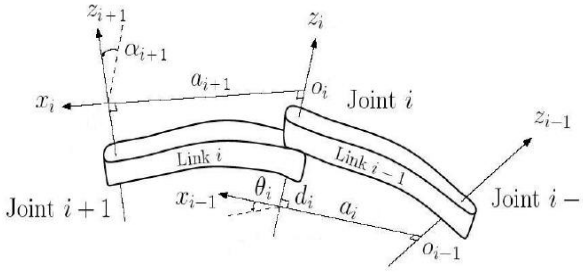

FIGURE 4.2D-H PARAMETERS OF A LINK I.E. $\theta_i, a_i, d_i, \alpha_i$

Step 8: The homogeneous transformation matrices A_i is determined by substituting theabove parameters as shown in equation.

Step 9: Then the global transformation matrix End0T is formed, as shown in equation.

This then gives the position and orientation of the tool frame expressed in base coordinates.

In this convention, each homogeneous transformation matrix i A is represented as aproduct of four basic transformations:

A_i Rot(z, θ_i)Trans(z, d_i)Trans(x, a_i)Rot(x , α_i)

$$= \begin{bmatrix} \cos(\theta_i) & -\sin(\theta_i)\cos(\alpha_i) & \sin(\theta_i)\sin(\alpha_i) & a_i\cos(\theta_i) \\ \sin(\theta_i) & \cos(\theta_i)\cos(\alpha_i) & -\cos(\theta_i)\sin(\alpha_i) & a_i\sin(\theta_i) \\ 0 & \sin(\alpha_i) & \cos(\alpha_i) & d_i \\ 0 & 0 & 0 & 1 \end{bmatrix}$$

Wherefour quantities θ_i, a_i, d_i, $\alpha_i$are parameter associate with link i and joint i. Thefour parameters θ_i, a_i, d_i, $\alpha_i$in the above equation are generally given name as joint angle,link length, link offset, and link twist.

4.3 THE FORWARD KINEMATICS OF A 5-DOF AND 7-DOF REDUNDANT MANIPULATOR.

4.3.1. Coordinate frame of a 5-DOF Redundant manipulator.

FIGURE 4.3 A PIONEER ARM REDUNDANT MANIPULATOR

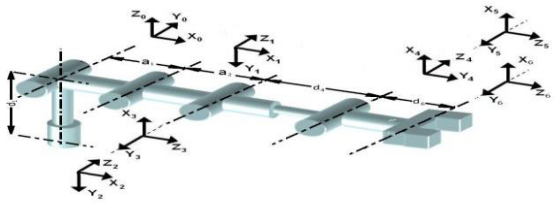

FIGURE 4.4 COORDINATE FRAME FOR THE 5-DOF REDUNDANT MANIPULATOR

TABLE 4.1 ANGLE OF ROTATION OF JOINTS

Types of Joint	Range of Rotation
Rotating base/ shoulder(θ_1)	0^0 to 180^0
Rotating elbow (θ_2)	0^0 to 180^0
Pivoting elbow (θ_3)	0^0 to 180^0
Rotating wrist (θ_4)	0^0 to 180^0
Pivoting wrist (θ_5)	0^0 to 180^0

4.3.2. FORWARD KINEMATICS CALCULATION OF THE 5-DOF REDUNDANT MANIPULATOR.

Robot control actions are executed in the joint coordinates while robot motions arespecified in the Cartesian coordinates. Conversion of the position and

orientation of a robotmanipulator end-effecter from Cartesian space to joint space is called as inverse kinematicsproblem, which is of fundamental importance in calculating desired joint angles for robotmanipulator design and control. The Denavit-Hartenberg (DH) notation and methodology is used to derive the kinematics of the 5-DOF Redundant manipulator. The coordinatesframe assignment and the DH parameters are depicted respectively where (x_4,y_4,z_4) represents the local coordinate frames at the five jointsrespectively (x_5,y_5,z_5) represents rotation coordinate frame at the end-effector where θirepresents rotation about the Z-axis and transition on about the X- axis, i d transition along theZ-axis, and i a transition along the X-axis.

TABLE 4.2 THE D-H PARAMETERS OF THE 5-DOF REDUNDANT MANIPULATOR.

Frame	θ_i (degree)	d_i (mm)	a_i (mm)	α_i (degree)
$O_0 - O_1$	θ_1	$d_1 = 130$	$a_1 = 70$	-90
$O_1 - O_2$	θ_2	0	$a_2 = 160$	0
$O_2 - O_3$	$-90 + \theta_3$	0	0	-90
$O_3 - O_4$	θ_4	$d_4 = 140$	0	90
$O_4 - O_5$	θ_5	0	0	-90
$O_5 - O_6$	0	$d_6 = 120$	0	0

The transformation matrix Ai between two neighboring frames and is expressedin equation (1) as,

A_i Rot(z,θ_i)Trans(z,d_i)Trans(x,a_i)Rot(x,α_i)

$$= \begin{bmatrix} \cos(\theta_i) & -\sin(\theta_i)\cos(\alpha_i) & \sin(\theta_i)\sin(\alpha_i) & a_i\cos(\theta_i) \\ \sin(\theta_i) & \cos(\theta_i)\cos(\alpha_i) & -\cos(\theta_i)\sin(\alpha_i) & a_i\sin(\theta_i) \\ 0 & \sin(\alpha_i) & \cos(\alpha_i) & d_i \\ 0 & 0 & 0 & 1 \end{bmatrix}$$

……..**1**

By substituting the D-H parameters in Table 4.1 into equation (1), it can be obtained the individual transformation matrices to and the general transformation matrix from the first joint to the last joint of the 5-DOF Redundant manipulator can be derived by multiplying all the individual transformation matrices ($^0T_6$).

$$^0T_6 = A_1A_2A_3A_4A_5A_6 = \begin{bmatrix} n_x & o_x & a_x & p_x \\ n_y & o_y & a_y & p_y \\ n_z & o_z & a_z & p_z \\ 0 & 0 & 0 & 1 \end{bmatrix}$$ ……..**2**

Where (P_x,P_y,P_z) are the positions (n_x,n_y,n_z), (o_x,o_y,o_z), (a_x,a_y,a_z) and are the orientations of the end-effector. The orientation and position of the end-effector can be calculated in terms of joint angles and the D-H parameters of the manipulator are shown in following matrix as:

$$\begin{bmatrix} c_1s_{23}c_4c_5 + s_1s_4c_5 + c_1c_{23}s_5 & -c_1s_{23}s_4 + s_1c_4 & -c_1s_{23}c_4s_5 - s_1s_4s_5 + c_1c_{23}c_5 & -d_6c_1s_{23}c_4s_5 - d_6s_1s_4s_5 + d_6c_1c_{23}c_5 + d_4c_1c_{23} + a_2c_1c_2 + a_1c_1 \\ s_1s_{23}c_4c_5 - c_1s_4c_5 + s_1c_{23}s_5 & -sls_{23}s_4 - c_1c_4 & -s_1s_{23}c_4s_5 + c_1s_4s_5 + s_1c_{23}c_5 & -d_6s_1s_{23}c_4s_5 + d_6c_1s_4s_5 + d_6s_1c_{23}c_5 + d_4s_1c_{23} + a_2s_1c_2 + a_1s_1 \\ c_{23}c_4c_5 - s_{23}s_5 & -c_{23}s_4 & -c_{23}c_4s_5 - s_{23}c_5 & -d_6c_{23}c_4s_5 - d_6s_{23}c_5 - d_4s_{23} - a_2s_2 + d_1 \\ 0 & 0 & 0 & 1 \end{bmatrix}$$ ….**3**

where $C_i = \cos(\theta_i)$,$S_i = \sin(\theta_i)$,$C_{23} = \cos(\theta_2+\theta_3)$ and $S_{23} = \sin(\theta_2+\theta_3)$ By equalizing the matrices in equations (2) and (3), the following equations are derived

$$p_x = -d_6c_1s_{23}c_4s_5 - d_6s_1s_4s_5 + d_6c_1c_{23}c_5 + d_4c_1c_{23} + a_2c_1c_2 + a_1c_1 \quad \textbf{4}$$

$$p_y = -d_6s_1s_{23}c_4s_5 + d_6c_1s_4s_5 + d_6s_1c_{23}c_5 + d_4s_1c_{23} + a_2s_1c_2 + a_1s_1$$

$$p_z = -d_6c_{23}c_4s_5 - d_6s_{23}c_5 - d_4s_{23}c_5 - d_4s_{23} - a_2s_2 + d_1$$

$$n_x = c_1s_{23}c_4c_5 + s_1s_4c_5 + c_1c_{23}s_5$$

$$n_y = s_1s_{23}c_4c_5 - c_1s_4c_5 + s_1c_{23}s_5$$

$$n_z = c_{23}c_4c_5 - s_{23}s_5$$

$$o_x = -c_1s_{23}s_4 + s_1c_4$$

$$o_y = -s_1s_{23}s_4 - c_1c_4$$

$$o_z = -c_{23}s_4$$

$$a_x = -c_1s_{23}c_4s_5 - s_1s_4c_5 + c_1c_{23}c_5$$

$$a_y = -s_1s_{23}c_4s_5 + c_1s_4s_5 + s_1c_{23}c_5$$

$$a_z = -c_{23}c_4s_5 - s_{23}c_5$$

……..**15**

From equation (4) to (15), the position and orientation of the 5-DOF Redundant manipulator end-effector can be calculated if all the joint angles are given. This is the solution to the forward kinematics.

4.3.3. Work space for the 5-DOF Redundant manipulator.

Considering all the D-H parameters, the x, y and z coordinates are calculated for 5-DOF Redundant

manipulator End-effector using forward kinematics equation shown in equations 4-15. For solving the forward kinematics equations, the angles of rotation of the joints are taken as tabulated in Table 4.1. Figure 4 shows the workspace for 5-DOF Redundant manipulator.

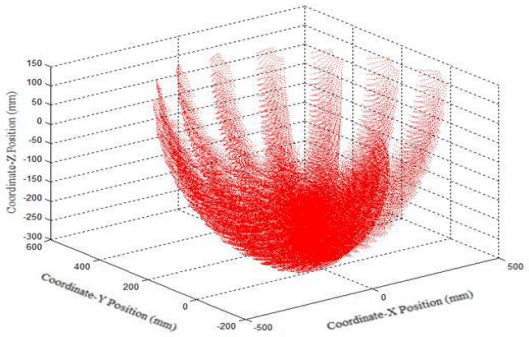

FIGURE 4.5 WORK SPACE FOR 5-DOF REDUNDANT MANIPULATOR

4.3.4. Coordinate frame of a 7-DOF Redundant manipulator

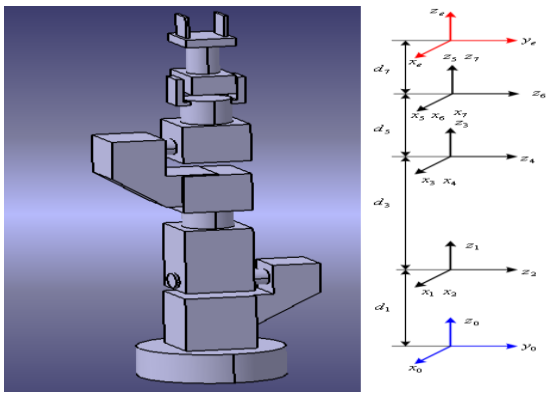

FIGURE 4.6 COORDINATE FRAME FOR A 7-DOF REDUNDANT MANIPULATOR

4.3.5. Forward kinematics calculation of the 7-DOF Redundant manipulator.

The D-H parameter for the 7-DOF Redundant manipulator is tabulated in Table 4.2.

TABLE 4.3. THE D-H PARAMETERS OF THE 7-DOF REDUNDANT MANIPULATOR

frame	Link	θ_i (degree)	d_i (cm)	a_i (cm)	α_i (degree)
O_0-O_1	1	θ_1=-270 to 270	d_1= 30	0	0
O_1-O_2	2	θ_2 = -110 to 110	0	0	-90
O_2-O_3	3	θ_3 = -110 to 110	d_3= 35	0	90
O_3-O_4	4	θ_4 = -110 to 110	0	0	-90
O_4-O_5	5	θ_5= -110 to 110	d_5= 31	0	90
O_5-O_6	6	θ_6= -110 to 110	0	0	-90
O_6-O_7	7	θ_7= -110 to 110	0	0	90
O_7-O_{end}	End	-	d_7= 31	0	0

By substituting the D-H parameters in Table 4.2 into equation (1), the individual transformation matrices A_1 to A_{End} can be obtained and the global transformation matrix ($^0T_{End}$) from the first joint to the last joint of the 7-DOF Redundant manipulator can be derived by multiplying all the individual transformation matrices. So,

$$^0T_{End} = A_1A_2A_3A_4A_5A_6A_7A_{End} = \begin{bmatrix} n_x & o_x & a_x & p_x \\ n_y & o_y & a_y & p_y \\ n_z & o_z & a_z & p_z \\ 0 & 0 & 0 & 1 \end{bmatrix}$$

Where P_x,P_y,P_z are the positions and (n_x,n_y,n_z), (o_x,o_y,o_z), (a_x,a_y,a_z) are the orientations of the end-effector. The orientation and position of the end-effector can be calculated in terms of joint angles and the D-H parameters of the manipulator are shown in following equations:

$$n_x = (c_7c_6c_5 - s_7s_5)\{c_3c_4(c_1c_2 - s_1s_2) - s_4(c_1s_2 + s_1c_2)\} + (c_7s_5c_6 + s_7c_5)\{s_3(s_1s_2 - c_1c_2)\} + s_6c_7\{c_3s_4(s_1s_2 - c_1c_2) - c_4(c_1s_2 + s_1c_2)\}$$

$$n_y = (c_7c_6c_5 - s_7s_5)\{c_3c_4(s_1c_2 + c_1s_2) + s_4(c_1c_2 - s_1s_2)\} + (c_7s_5c_6 + s_7c_5)\{-s_3(s_1c_2 + c_1s_2)\} + s_6c_7\{-c_3s_4(s_1c_2 + c_1s_2) + c_4(c_1c_2 - s_1s_2)\}$$

$$n_z = c_7c_6s_3c_4s_5 - c_7c_6s_5c_3 + c_7s_6s_3c_3 + c_7s_6s_3s_4 + s_7c_3c_5 - s_7s_3c_4s_5$$

$$o_x = c_6\{c_3s_4(s_1s_2 - c_1c_2) - c_4(c_1s_2 + s_1c_2)\} - s_6c_5\{c_3c_4(c_1c_2 - s_1s_2) - s_4(c_1s_2 + s_1c_2)\} - s_6s_5\{s_3(s_1s_2 - c_1c_2)\}$$

$$o_y = c_6\{-c_3s_4(s_1c_2 + c_1s_2) + c_4(c_1c_2 - s_1s_2)\} - s_6c_5\{c_3c_4(s_1c_2 + c_1s_2) + s_4(c_1c_2 - s_1s_2)\} - s_6s_5\{-s_3(s_1c_2 + c_1s_2)\}$$

$$o_z = s_6s_3c_4c_5 + s_5c_3s_6 + s_3c_4c_6$$

$$a_x = (s_7c_6c_5 + c_7s_5)\{c_3c_4(c_1c_2 - s_1s_2) - s_4(c_1s_2 + s_1c_2)\} + (s_7s_5c_6 - c_7c_5)\{s_3(s_1s_2 - c_1c_2)\} + s_6s_7\{c_3s_4(s_1s_2 - c_1c_2) - c_4(c_1s_2 + s_1c_2)\}$$

$$a_y = (s_7c_6c_5 + c_7s_5)\{c_3c_4(s_1c_2 + c_1s_2) + s_4(c_1c_2 - s_1s_2)\} + (s_7c_6s_5 - c_7c_5)\{-s_3(s_1c_2 + c_1s_2)\} + s_7s_6\{-c_3s_4(s_1c_2 + c_1s_2) + c_4(c_1c_2 - s_1s_2)\}$$

$$a_z = s_7c_6s_3c_4c_5 - s_7c_6s_5c_3 + s_7s_6s_4s_3 + c_7c_4s_3s_5 - c_3c_5c_7$$

$$p_x = \{d_7(s_7c_6c_5 + c_7s_5)\}\{c_3c_4(c_1c_2 - s_1s_2) - s_4(c_1s_2 + s_1c_2)\} + \{d_7(s_7s_5c_6 - c_7c_5)\}\{s_3(s_1s_2 - c_1c_2)\} + (d_7s_7s_6 + d_5)\{c_3s_4(s_1s_2 - c_1c_2) - c_4(c_1s_2 + s_1c_2)\} + \{-d_3(c_1s_2 + s_1c_2)\}$$

$$p_y = \{d_7(s_7c_6c_5 + s_5c_7)\}\{c_3c_4(s_1c_2 + c_1s_2) + s_4(c_1c_2 - s_1s_2)\} + \{d_7(s_7s_5c_6 - c_7c_5)\}\{-s_3(s_1c_2 + c_1s_2)\} + (d_7s_7s_6 + d_5)\{-c_3s_4(s_1c_2 + c_1s_2) + c_4(c_1c_2 - s_1s_2)\}$$

$$p_z = d_7s_7s_3c_6c_5c_4 - d_7s_7s_5c_6c_3 + d_7s_7s_6s_4s_3 + d_7s_5s_3c_7c_4 - d_7c_7c_5c_3 + d_5s_4s_3 + d_1$$

……28

From equation (17)-(28), are the position and orientation of the 7-DOF Redundant manipulator end-effector and the exact value of these equations can be calculated if all the joint angles are given. This is the solution to the forward kinematics.

4.3.6. WORK SPACE FOR THE 7-DOF REDUNDANT MANIPULATOR

Considering all the D-H parameters, the x, y and z coordinates (i.e. End-effector coordinates) are calculated for 7-DOF Redundant manipulator using forward kinematics equation as shown in equations 17-28. For solving the forward kinematics equations, the angles of rotation of the joints are taken as tabulated in Table 4.2. Figure 4.6 shows the workspace for this manipulator.

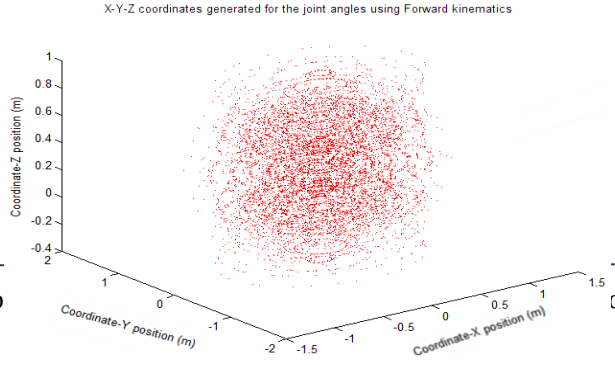

FIGURE 4.7 WORK SPACE FOR 7-DOF REDUNDANT MANIPULATOR

4.4 INVERSE KINEMATICS OF 5-DOF REDUNDANT MANIPULATOR.

The forward kinematics equations (4)-(15) are highly nonlinear and discontinuous. It isobvious that the inverse kinematics solution is very difficult to derive. This paper usesvarious tricky strategies to solve the inverse kinematics of the 5-DOF robot manipulator.

From equations (4) and (13), the following equation is derived:

$$p_x - d_6a_x = c_1(d_4c_{23} + a_2c_2 + a_1) \quad \ldots\ldots \mathbf{29}$$

Similarly by manipulating in similar way from equations (5) and (14), the following equation is derived as:

$$p_y - d_6a_y = s_1(d_4c_{23} + a_2c_2 + a_1) \quad \ldots\ldots\ldots\ldots \mathbf{30}$$

It can be noted that the values of θ_2 andθ_3 in 5-DOF Redundant manipulator onlytakes integral values in a limited range. By checking all possible joint angles θ_2 and$\theta_3$that $(d_4c_{23}+a_2c_2+a_1) \neq 0$holds good, which means that p_x-d_6a_x and p_y- $d_6a_y$will notequals to zero at same time. Now considering the two possible situations,

If $(d_4c_{23} + a_2c_2a_1) > 0$, the solution for θ_1 is,

$$\theta_1 = a\tan 2p_y - d_6a_y, p_x - d_6a_x)$$

$$\theta_1 = a\tan 2d_6a_y - p_y, d_6a_x - p_x)$$

….**32**

In solving the inverse kinematics solution of a higher DOF robot, atan^{-1}function cannot show the effect of the individual sign for numerator and denominator but represent the angle in first or fourth quadrant. To overcome this problem and determine the joint in the correct quadrant, atan2 function is introduced in equations (31) and (32).

Now for deriving solutions forθ_2 andθ_3, equations (29) and (30) can be represented as follows:

$$d_4c_{23} + a_2c_2 = (p_x - d_6a_x)/c_1 - a_1$$

$$d_4c_{23} + a_2c_2 = (p_y - d_6a_y)/s_1 - a_1 \quad \text{.....34}$$

From equations (6) and (15), the following equation can be derived,

$$p_z - d_6a_z = -d_4s_{23} - a_2s_2 + d_1 \quad \text{.....35}$$

Now considering equations (33) and (35),

$$r = (p_x - d_6a_x)/c_1 - a_1$$

$$r_z = -d_4s_{23} - a_2s_2 + d_1 \quad \text{.....37}$$

Now squaring the equations (36) and (37) followed by addition, equation (38) can be derived as follows:

$$d_4^2 + 2a_2d_4(c_2c_{23} + s_2s_{23}) + a_2^2 = r + r_z^2 \quad \text{.....38}$$

Solving the terms $C_2C_{23}+S_2S_{23}$ in equation 38 we get

$$(c_2c_{23} + s_2s_{23}) = \cos\theta_3 = -\cos(\theta_3 - \pi) = \cos(-\theta_3) = -\cos(\pi - \theta_3)$$

Therefore, there are several possible solutions for θ_3 , which are as follows:

$$\theta_3 = \pm a\cos\left(\frac{r^2 + r_z^2 - a_2^2 - d_4^2}{2a_2d_4}\right)$$

$$\theta_3 = \pm\left[\pi - a\cos\left(\frac{a_2^2 - d_4^2 - r^2 + r_z^2}{2a_2d_4}\right)\right] \quad \text{...40}$$

Where the positive sign on the right hand side of the equation denotes for the elbow-out and the negative sign represents elbow-in configuration. The two solutions for the elbow-out and elbow-in of the 5-DOF Redundant manipulator are shown in the Figure 4.7.

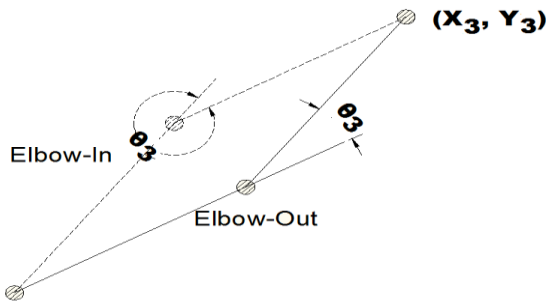

FIGURE 4.8 ELBOW –IN AND ELBOW-OUT CONFIGURATION

Now consider the possible solutions for θ_2

For the sake of convenience, equation (35) can be rewritten as equation (41)

$$d_4s_{23} = B_1 - a_2s_2 \quad \text{.....41}$$

Where,

$$d_6a_z - p_z + d_1 = B_1$$

Considering the equations (33) and (34), equation (42) is derived as:

$$d_4c_{23} + a_2c_2 = \pm\sqrt{(-a_xd_6 + p_x)^2 + (-a_yd_6 + p_y)^2} \quad \text{...42}$$

$$\text{Let } B_2 = \pm\sqrt{(-a_xd_6 + p_x)^2(-a_yd_6 + p_y)^2},$$

$$d_4c_{23} = B_2 - a_2c_2 \quad \text{...43}$$

Rearranging equations (41) and (43) and solving for B_1 and B_2. Equations (44) and (45) are derived as:

$$B_1 = (d_4c_3 + a_2)s_2 + (d_4s_3)c_2$$

$$B_2 = (d_4c_3 + a_2)c_2 - (d_4s_3)s_2 \quad \text{..... 45}$$

Dividing both sides of (44) and (45), by $\sqrt{B_1^2 + B_2^2}$, equations (46) and (47) are derived as,

$$\cos\theta * \sin\theta_2 + \sin\theta * \cos\theta_2 = \frac{B_1}{\sqrt{B_1^2 + B_2^2}}$$

$$\cos\theta * \sin\theta_2 - \sin\theta * \cos\theta_2 = \frac{B_2}{\sqrt{B_1^2 + B_2^2}} \quad \text{...47}$$

Where,

$$\cos\theta = \frac{(d_4c_3 + a_2)}{\sqrt{B_1^2 + B_2^2}}$$

$$\sin\theta = \frac{(d_4s_3)}{\sqrt{B_1^2 + B_2^2}}$$

The equations (46) and (47) are rewritten as:

$$\sin(\theta + \theta_2) = \frac{B_1}{\sqrt{B_1^2 + B_2^2}} \quad \text{.....48}$$

$$\cos(\theta+\theta_2)=\frac{B_2}{\sqrt{B_1^2+B_2^2}} \quad \text{.....49}$$

Therefore,$\theta+\theta 2 = a\tan 2(B_1+B_2)+ 2m\mu$ and

$$\theta=\pm a\cos\frac{(d_4c_3+a_2)}{\sqrt{B_1^2+B_2^2}}$$

Where m = -1, 0 or +1. It is clear that θ could be in [0, π] or [-π,0]. The range of θ depends on the range depends on the range ofθ_3. Therefore, if $0\le\theta_3\le\pi$, then$S_3>0$and sin(θ)<0, thus$0\le\theta\le\pi$. Then θ_2 can be derived as:

$$\theta_2=a\tan 2(B_1,B_2)-a\cos\frac{(d_4c_3+a_2)}{\sqrt{B_1^2+B_2^2}}+2m\pi \quad \text{...50}$$

Otherwise - $\pi<\theta_3<0$ if, then$S_3<0$ and$\sin\theta<0$thus. Then - $\pi<\theta<0$ the next possible solution forθ_2 is as:

$$\theta_2=a\tan 2(B_1,B_2)+a\cos\frac{(d_4c_3+a_2)}{\sqrt{B_1^2+B_2^2}}+2m\pi$$

.51

Now thatθ_1,θ_2 andθ_3 are known, the solutions forθ_4 andθ_5 can be found by using the remaining forward kinematics equations.

Considering the equation (12), the value of

$$s_4=-\frac{o_z}{c_{23}} \quad \text{.....52}$$

When, $C_{23}\neq 0$

Similarly, from the equations (10) and (11), the possible solution for C_4 is derived as:

$$c_4=\frac{(o_x-c_1s_{23}o_z/c_{23})}{s_1}$$

$$c_4=\frac{-(o_y-s_1s_{23}o_z/c_{23})}{c_1} \quad \text{..... (53)(54)}$$

Using equation (53) and (54) for small value of C_1, the solution forθ_4 is

$$\theta_4=a\tan 2\left(-\frac{o_z}{c_{23}},\frac{(o_z-c_1s_{23}o_z/c_{23})}{s_1}\right)$$

$$,\quad \theta_4=a\tan 2\left(-\frac{o_z}{c_{23}},\frac{-(o_y-s_1s_{23}o_z/c_{23})}{c_1}\right)$$

... (55)(56)

Now for solution of, considering equation (9), the value of

$$c_5=\frac{n_z+s_{23}s_5}{c_{23}c_4} \quad \text{.....57}$$

Similarly the value of is derived by using equation (15) i.e.,

$$s_5=-\frac{a_z+s_{23}c_5}{c_{23}c_4} \quad \text{.....58}$$

using equation (41) in (40) and vice versa, the term C_5 and S_5 is rewritten as:

$$c_5=\frac{n_zc_{23}c_4-s_{23}a_z}{c_{23}^2c_4^2+s_{23}^2} \quad \text{and} \quad s_5=-\frac{(a_zc_{23}c_4+s_{23}n_z)}{c_{23}^2c_4^2+s_{23}^2}$$

Now using this above derivation of and , is derived as follows:

$$\theta_5=a\tan 2\{-(a_zc_{23}c_4+s_{23}n_z),(n_zc_{23}c_4-s_{23}a_z)\} \quad \text{.....59}$$

The above derivations with various conditions being taken into account provide acomplete analytical solution to inverse kinematics of 5-DOF Redundant manipulator. It is tobe noted that there exist two possible solutions for θ_1, $\theta_2,\theta_3,\theta_4$depicted in (31) or (32), (50)or (51), (39) or (40), (55) or (56) respectively. So to know which solution holds good to studythe inverse kinematics, all joint angles are obtained and compared using the forwardkinematics solution. This process is being applied forθ_1, $\theta_2,\theta_3,\theta_4$to choose the correctsolution, all the four sets of possible solutions (joint angles) calculated, which generate fourpossible corresponding positions and orientations using the forward kinematics. Bycomparing the errors between these four generated positions and orientations and the givenposition and orientation, one set of joint

angles, which produces the minimum error, is chosenas the correct solution. The solutions (32), (50), (39), and (56) holds correct for obtaining the values of θ_1, θ_2,θ_3,$\theta_4$respectively.

4.5 ANFIS Architecture used for 5-DOF Redundant manipulator.

The coordinates and the angles obtained from forward kinematics solutions are used as training data to train ANFIS network with the triangular membership function with a hybrid learning algorithm. For solving the inverse kinematics equation of 5-DOF Redundant manipulator, in this work, considers the ANFIS structure with first order Sugeno model containing 343 rules. For the neuro-fuzzy model used in this work, 1024 data points analytically obtained using forward kinematics, of which 776 are used for training and the remaining 248 are used for testing (or validating).

Training of ANFIS is usually performed by using ANFIS editor GUI of MATLAB [64]. The ANFIS Editor GUI window displays the four main sub displays. These are 1. Load data, 2. Generate FIS, 3. Train FIS and 4. Test FIS. Once the FIS is generated, the model structure can be viewed as shown in Figure.

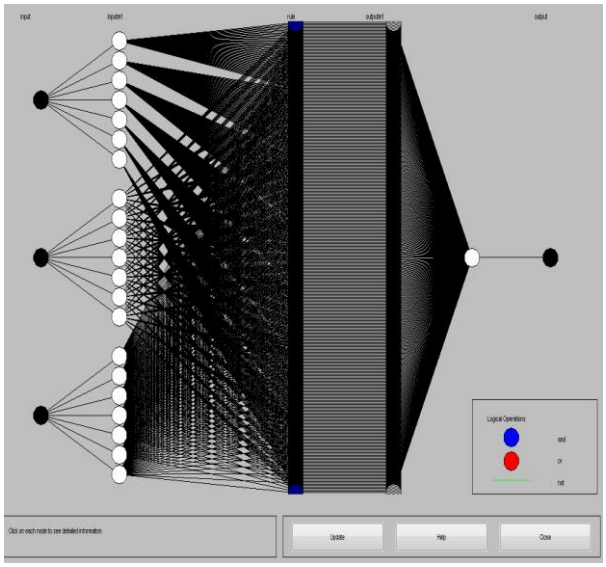

FIGURE 4.9 ANFIS MODEL STRUCTURE USED FOR 5-DOF REDUNDANT MANIPULATOR

The branches in Figure are color coded. Color coding of branches characterize the rules and indicate whether *and*, *or*, *not* are used in the rules. The input is represented by the left-most node and the output by the right-most node. The node represents a normalization factor for the rules. Clicking on the nodes indicates information about the structure. To start the training, GENFIS1 function is used. GENFIS1 uses the grid partitioning and it generates rules by enumerating all possible combinations of membership functions of all inputs; this leads to an exponential explosion even when the number of inputs is moderately large. For instance, for a fuzzy inference system with 3 inputs, each with seven membership functions, the grid partitioning leads to 343 (=7^3) rules. GENFIS1 use a given training data set to generate an initial fuzzy inference system (represented by a FIS matrix) that can be fine-tuned via the ANFIS command. GENFIS1 produces a grid partitioning of the input space and a fuzzy inference system where each rule has zero coefficients in its output equation.

4.6 ANFIS Architecture used for 7-DOF Redundant manipulator.

For solving the inverse kinematics equation of 7-DOF Redundant manipulator, in this work, the grid partitioning option in the ANFIS toolbox is used. For each input, 7 membership function (Gaussian membership) are used along with 343(=7^3) fuzzy rules are applied for all three inputs. For the

neuro-fuzzy model used, 2187 data points are analytically obtained from MATLAB, of which 1640 are used for training and the remaining 547 are used for testing (validating). The model structure for the 7-DOF Redundant manipulator used in ANFIS can be viewed as similar to the structure obtained for 5-DOF Redundant manipulator as discussed in the previous section. For obtaining the model for 7-DOF Redundant manipulator the Gaussian membership function with seven number of membership for each input is used as shown in following figure 14. The model structure obtained for 7-DOF manipulator. The

Anfis information used for solving the 7-DOF Redundant manipulator for this work is tabulated in Table. 4.

TABLE 4.4 ANFIS INFORMATION USED FOR SOLVING 7-DOF REDUNDANT MANIPULATOR

3 inputs	: Cartesian coordinates: x, y, and z
1 output	: joint coordinate (θ)
7 member functions each input node	: Sugeno types
Number of nodes	: 734
Number of linear parameters	: 1372
Number of nonlinear parameters	: 42
Total number of parameters	: 1414
Number of training data pairs	: 1638
Number of checking data pairs	: 2187
Number of fuzzy rules	: 343

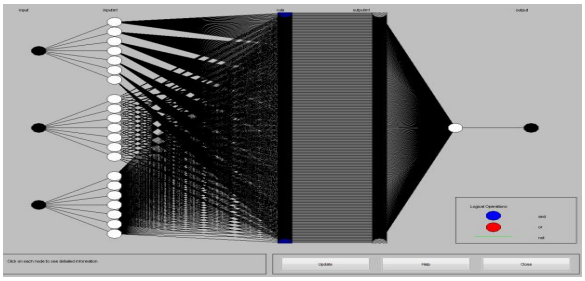

FIGURE 4.10 ANFIS MODEL STRUCTURE USED FOR 5-DOF REDUNDANT MANIPULATOR

V. RESULT AND DISCUSSION

In this section of the thesis the surface plots, the residual plots and the normal probabilityplots for the 5-DOF and 7-DOF redundant manipulator is carried out. The surface plotsobtained for this type of manipulators explains the efficiency of the ANFIS methodology.

The residual plots obtained by comparing the predicted data from the ANFIS and theanalytical data show that, the data predicted using ANFIS methodology deviate very lessfrom the analytical data. The last section of this chapter is concluded with obtaining thenormal probability plots. The details of the plots are explained in the following section.

5.1 3-D SURFACE VIEWER ANALYSIS

In this section the 3-D surface plots, obtained for the 5-DOF and 7-DOF Redundantmanipulator is discussed. The surface plotsdisplay both the connecting lines and faces of thesurface in color. The surf command in MATLAB tool is use to create the 3-D surface plots ofthe matrix data. The surface plot explains the relation between the output and two inputs.

5.1.1 3-D Surface plots obtained for all joint angles of 5-DOF Redundant manipulator

Figures 15-19 show surface plot of five ANFIS networks relating inputs with joint anglesof 5-DOF Redundant manipulator. Figure 15 indicates the surface plot between Cartesian coordinates y and z for θ_1. It shows that when the values of y and z moving in a positivedirection, there is a marginal increase followed by a decrease inθ_1 values. The inputs-outputsurface plot of θ_2 is shown in Figure 16. The Figure depicts that the value of θ_2 increaseslinearly when moving in the positive direction of y coordinate to some values of y and thenthere is a sudden increase of θ_2 values. No significant change in the value of θ_2 is observedwith change in values of z coordinate. By moving from negative direction to the positivedirection of x and y coordinates, the θ_3 value decreases first then followed by slightlyincrease, can be easily conclude from figure 5.2 Similarly the surface plot of θ_5 with inputvariables x and z

coordinate is depicted in figure 5.4 It shows that the value of inputs hassignificant effect in determining the value of θ_5. It concludes from the surface plot that thecontribution of interdependent parameters toward obtaining the output can easily providethrough the ANFIS algorithm and can be hardly obtained otherwise without employing massive computations. All the surface viewer plots show that the total surface is covered by the rule base.

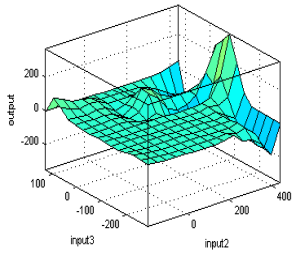

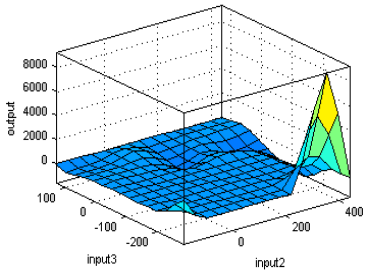

FIGURE 5.1 SURFACE PLOT FOR θ_1 FIGURE 5.2 SURFACE PLOT FOR θ_2

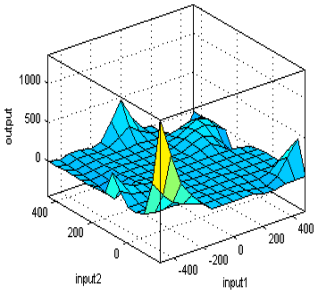

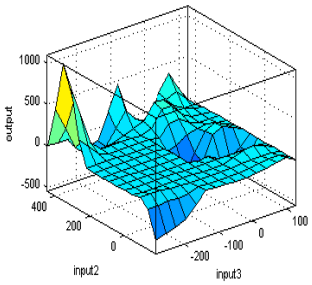

FIGURE 5.3 SURFACE PLOT FOR θ_3 IGURE 5.4 SURFACE PLOT FOR θ_4

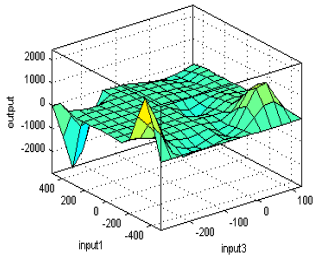

FIGURE 5.5 SURFACE PLOT FOR θ_5

5.1.2 3-D Surface plots obtained for all joint angles of 7-DOF Redundant manipulator

The following Figure 5.4-5.10 shows the three dimensional surface plot of ANFIS networkrelating to the joint angle of 7-DOF Redundant manipulator. Figure 19 indicates the surfaceplot between Cartesian coordinates y and z for θ_1. When the value of z decreases, there is asudden increase in θ_1 value followed by decrease at the middle range of z value and there isno significant change in θ_1 value for y coordinate. The inputs-output surface plot of θ_2 isshown in Figure 20. The Figure depicts that the value of θ_2 decrease first followed byincrease, for the increase in the value of z. No significant change in the value of θ_2 isobserved with change in values of y coordinate. When y changes from positive value tonegative value, there is a marginal increase in the value of θ_3 as well as there is nosignificant change with the value of z, as clearly noticed from Figure 5.6. With the increase iny value, at its middle range, the value of θ_5 decrease first then increase, where as there is no significant change for values of z, as depicted in Figure 5.8 Similarly, the 3 dimensional surface viewer for can be explain.All the surface plots obtained from ANFIS, are continuous, smooth and the total surface is covered by the rule base.

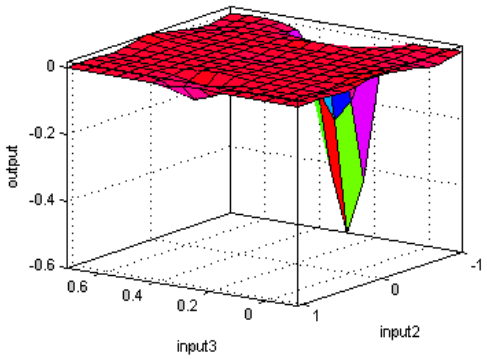

FIGURE 5.6 SURFACE PLOT FOR θ_2

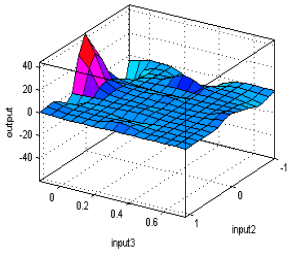

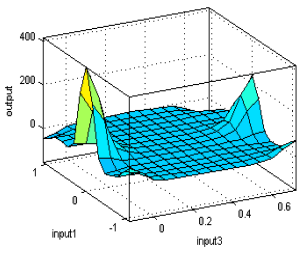

FIGURE 5.7 SURFACE PLOT FORθ_3 FIGURE 5.8 SURFACE PLOT FOR θ_4

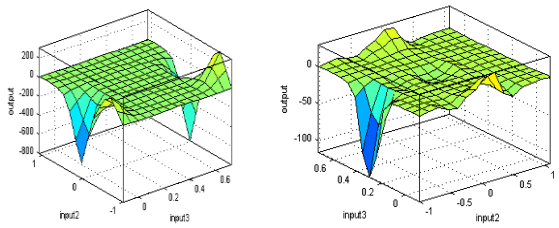

FIGURE 5.9 SURFACE PLOT FOR θ_5FIGURE 5.10 SURFACE PLOT FOR θ_6

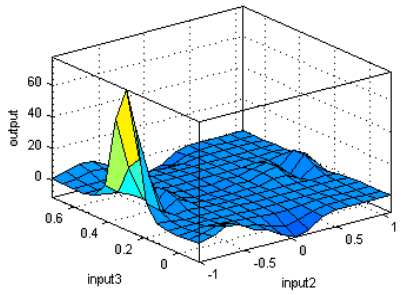

FIGURE 5.11 SURFACE PLOTS FOR θ_7

5.2 RESIDUAL PLOT ANALYSIS

Residuals are the difference between the predicted output from the model (ANFIS) and the actual values of joint angles. The residual plot is a graph that shows the residuals in the vertical axis and the independent variables in the horizontal axis. If the points in the residual plot are randomly dispersed around the horizontal axis, the prediction model is considered to be appropriate for the data i.e. there is no drift in the data. In this section the residual plots are obtained for training and testing data of all joint angles of 5-DOF Redundant manipulator. It depicts the distribution of residuals of all joint angles are in the positive and negative axis of the plot. The residual plots for 5-DOF and 7-DOF are shown in following section.

5.2.1 The Residual plot of Training data for all joint angle of 5-DOF Redundantmanipulator.

The residual plots of training data for θ_1 ,θ_2 ,θ_3 ,θ_4 and θ_5 of 5-DOF Redundant robotmanipulator are depicted in Figures 5.11-5.15 respectively. The residual plot shows a fairlyrandom pattern as some of the residuals are in positive and some are lies in the negative sideof the horizontal axis. Figure 27 shows a random pattern indicating a good fit for trainingdata of θ_1. As a very large number of residuals lie close to the horizontal axis shown inFigure 28, it indicates a reasonably good fit for θ_2 . The Figures 5.13-5.14 indicates a decent fitto the model of θ_3 and θ_4 as most of the residuals lie between -0.01 to 0.01. The Figure 5.15explains the residual plot for training data of θ_5. It indicates a few of the residuals of 5 θliesbeyond the range -0.1 to 0.1 and does not alter the prediction model of the data. The averageabsolute error (actual minus and predicted values) for the training data are found to be0.0700, 0.0011, 0.0330, 0.0850, and 0.0240 for the joint coordinates θ_1,θ_2,θ_3,θ_4 and $\theta_5$respectively. Similarly, the average absolute error of the testing data for the joint coordinatesθ_1,θ_2,θ_3 ,θ_4 and $\theta_5$are found to be 0.06, 0.03, 0.09,0.10, and 0.11 respectively.

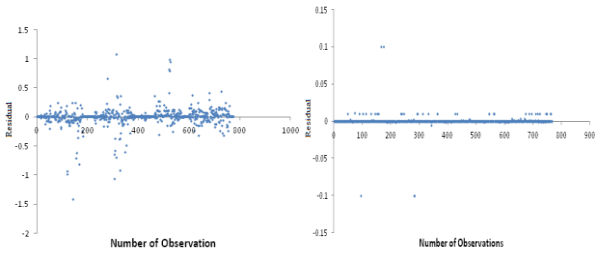

FIGURE 5.12 RESIDUAL PLOT OF TRAINING DATA FOR θ_1

FIGURE 5.13 RESIDUAL PLOT OF TRAINING DATA FOR θ_2

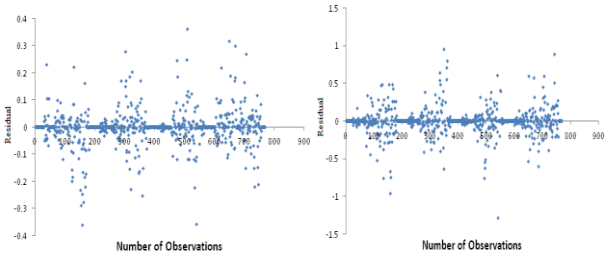

FIGURE 5.14 RESIDUAL PLOT OF TRAINING DATA FOR θ_3

FIGURE 5.15 RESIDUAL PLOT OF TRAINING DATA FOR θ_4

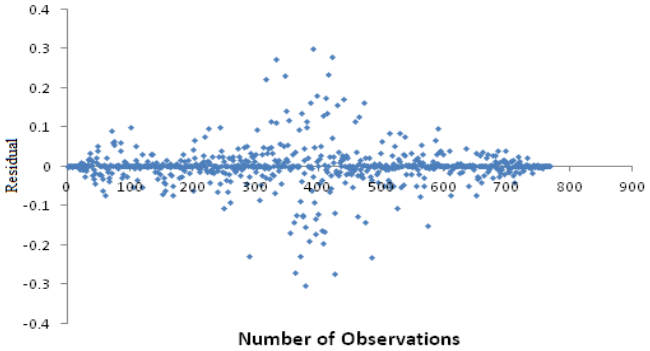

FIGURE 5.16 RESIDUAL PLOT OF TRAINING DATA FORθ_5

5.2.2 The Residual plot of testing data for all joint angle of 5-DOF Redundantmanipulator.

The residual plots of testing data for θ_1, $\theta 2$, $\theta 3$; $\theta 4$ and $\theta_5$of 5-DOF Redundant robotmanipulator are studied. The residual plot shows a fairly random pattern as some of theresiduals are in positive axis and some are lies in the negative axis of the of the graph. Figure32 shows a random pattern indicating a good fit for training data of θ_1. As a very largenumber of residuals lie close to the horizontal axis shown in Figure 5.16, it indicates areasonably good fit for θ_2. The residuals for θ_3 lie between -0.2 to 0.2 and distributed overboth sides of the mean line. It indicates that the prediction model is well suited for the studyFigure 5.14. The Figures 5.19-5.20 indicates a decent fit to the model of 4 θ and 5 θ as most of theresiduals lie between -0.03 to 0.03.

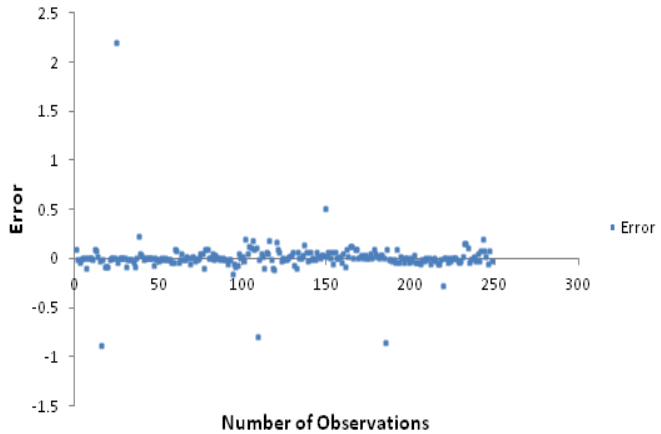

FIGURE 5.17 RESIDUAL PLOT OF TESTING DATA FOR θ_1

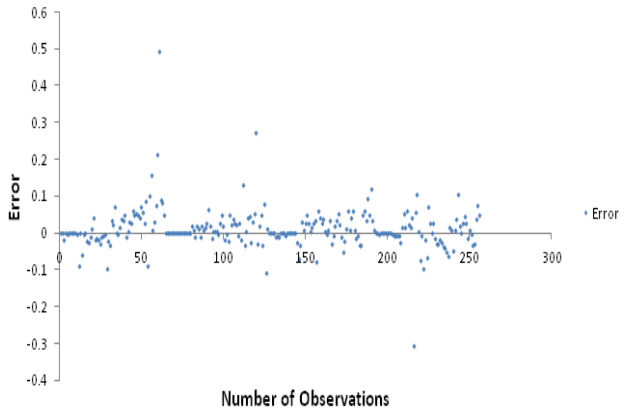

FIGURE 5.18 RESIDUAL PLOT OF TESTING DATA FOR θ_2

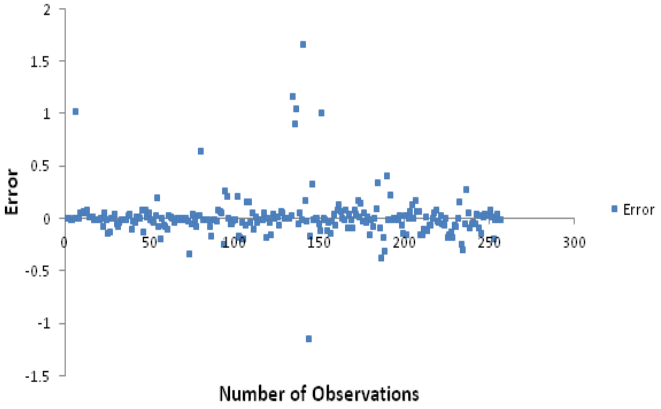

FIGURE 5.19 RESIDUAL PLOT OF TESTING DATA FOR θ_3

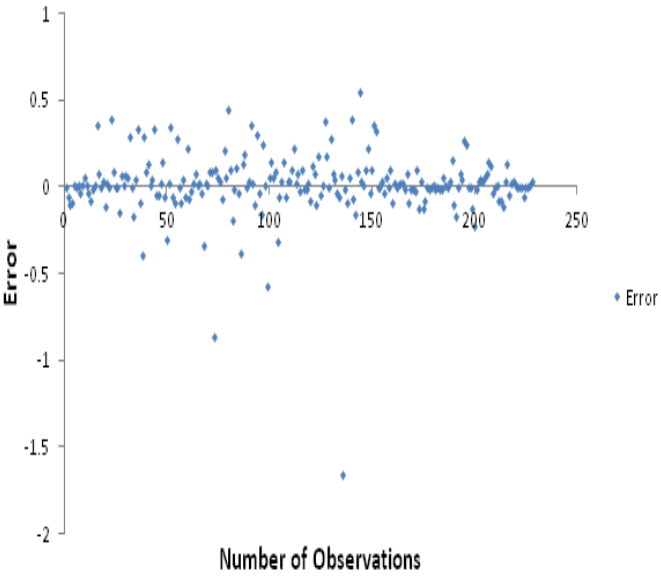

FIGURE 5.20 RESIDUAL PLOT OF TESTING DATA FORθ_4

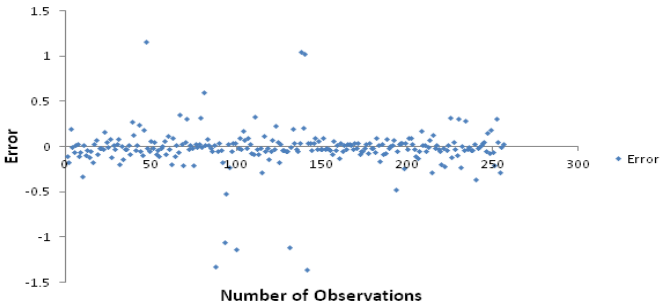

FIGURE 5.21 RESIDUAL PLOT OF TESTING DATA FOR θ_5

5.2.3 The Residual plot of Training data for all joint angle of 7-DOF Redundantmanipulator.

Similarly the residual plots of training data for θ_1, $\theta 2$, $\theta 3$; $\theta 4$ and $\theta_5$of 7-DOFredundant robot manipulator are studied. The residual plot shows a fairly random pattern assome of the residuals are in positive and some are lies in the negative side of the horizontalaxis. Figure 5.12 shows a random pattern indicating a good fit for training data of θ_1. As a verylarge number of residuals lie close to the horizontal axis shown in Figure 5.22, it indicates areasonably good fit forθ_2. The Figures 5.23-5.24 indicates a decent fit to the model of 3 θ and4 θ as most of the residuals lie between -0.01 to 0.01. The Figure 5.25 explains the residualplot for training data of θ_5. It indicates a few of the residuals of θ_5 lies beyond the range -0.1to 0.1 and does not alter the prediction model of the data. The residual plots of training datafor θ_6, θ_7 are depicted in Figure 5.26 and Figure 5.27.

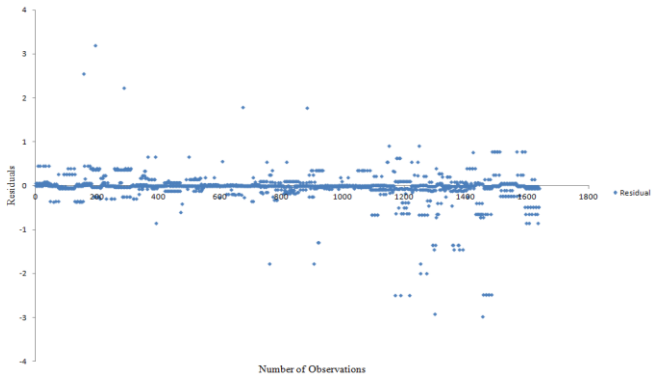

FIGURE 5.22 RESIDUAL PLOT OF TRAINING DATA FOR θ_1

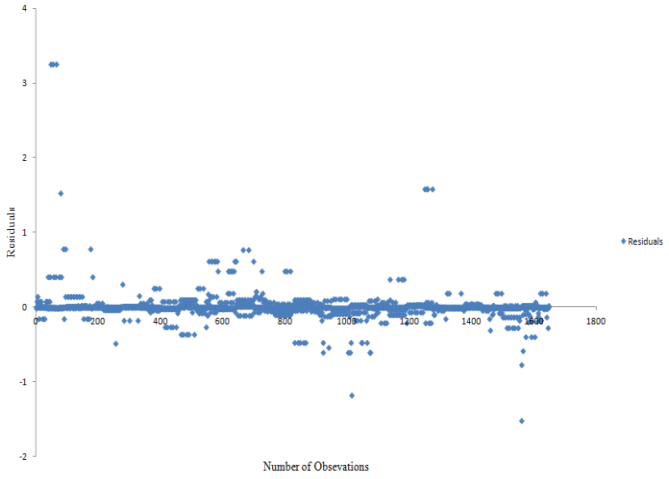

FIGURE 5.23 RESIDUAL PLOT OF TRAINING DATA FOR θ_2

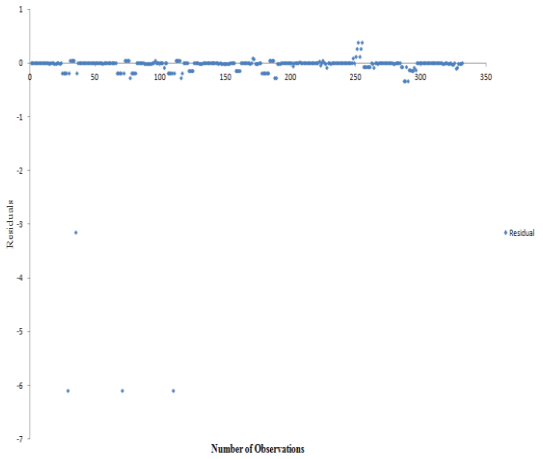

FIGURE 5.24 RESIDUAL PLOT OF TRAINING DATA FOR θ_3

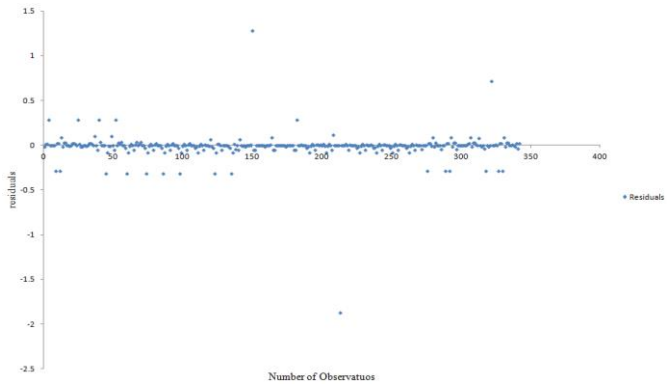

FIGURE 5.25 RESIDUAL PLOT OF TRAINING DATA FOR θ_4

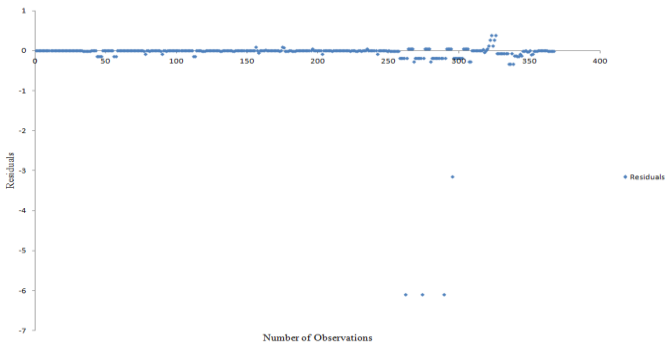

FIGURE 5.26 RESIDUAL PLOT OF TRAINING DATA FOR θ_5

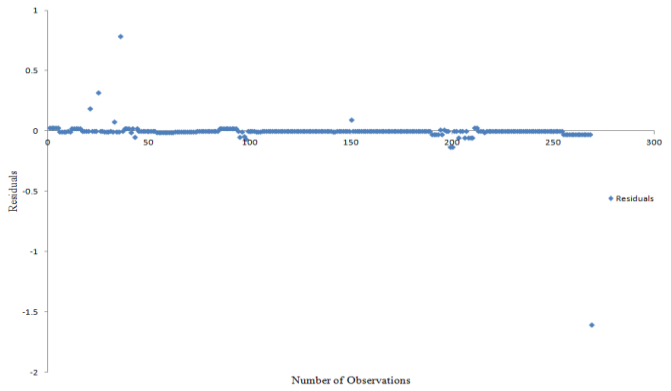

FIGURE5.27 RESIDUAL PLOT OF TRAINING DATA FORθ_6

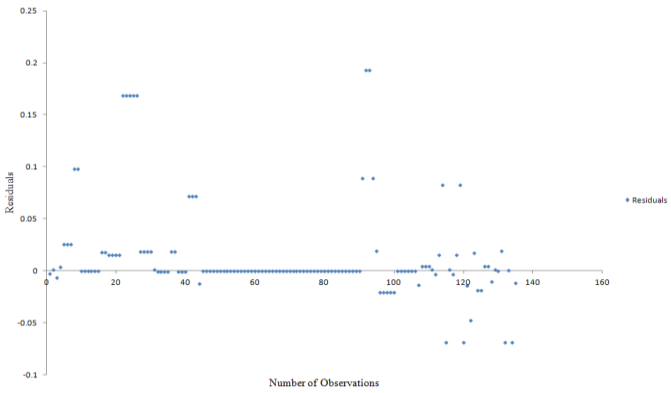

FIGURE 5.28 RESIDUAL PLOT OF TRAINING DATA FOR θ_7

5.2.4 The Residual plot of testing data for all joint angle of 7-DOF Redundantmanipulator.

The residual plots of testing data for θ_1, $\theta 2$, $\theta 3$, $\theta 4$ and $\theta_5$of 7-DOF redundantrobot manipulator are studied.The residual plot shows a fairly random pattern as some of theresiduals are in positive axis and some are lies in the negative axis of the of the graph. Figure5.16 shows a random pattern indicating a good fit for training data of θ_1. As a very largenumber of residuals lie close to the horizontal axis shown in Figure 5.17 it indicates areasonably good fit for θ_2. The residuals for θ_3 lie between -0.2 to 0.2 and distributed overboth sides of the mean line. It indicates that the prediction model is well suited for the studyfigure 5.18. The Figures 5.19-5.20 indicates a decent fit to the model of θ_4 and θ_5 as most of theresiduals lie between -0.03 to 0.03. The residual plot of θ_6 and $\theta_7$are presented in Figure 5.31and Figure 5.32.

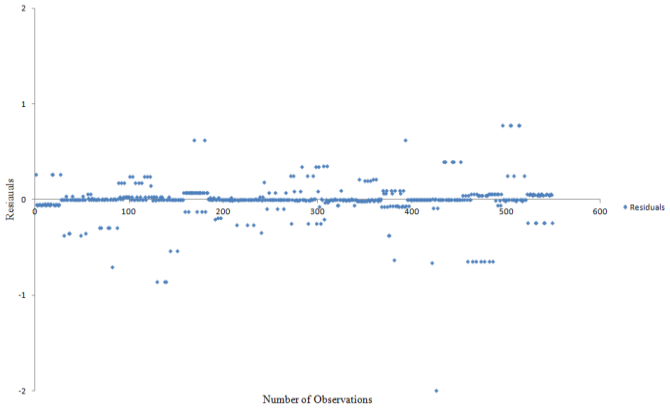

FIGURE 5.29 RESIDUAL PLOT OF TESTING DATA FORθ_1

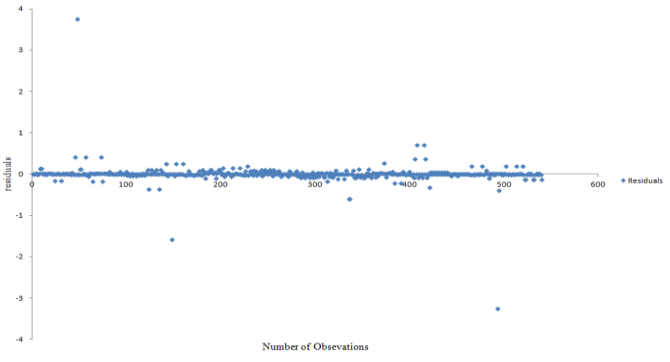

FIGURE 5.30 RESIDUAL PLOT OF TESTING DATA FOR θ_2

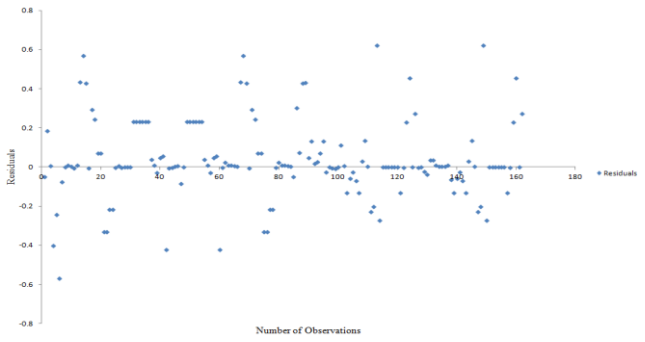

FIGURE 5.31 RESIDUAL PLOT OF TESTING DATA FOR θ_3

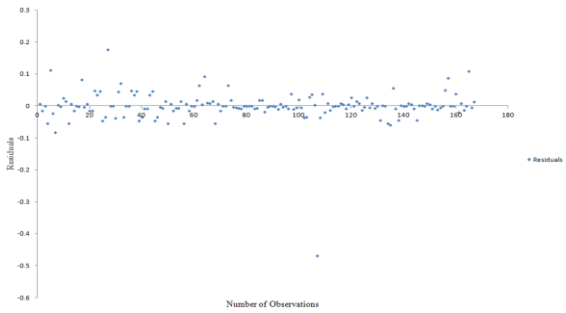

FIGURE 5.32 RESIDUAL PLOT OF TESTING DATA FOR θ_4

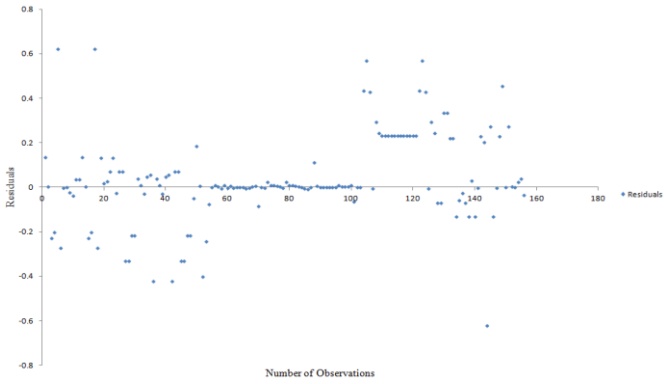

FIGURE 5.33 RESIDUAL PLOT OF TESTING DATA FOR θ_5

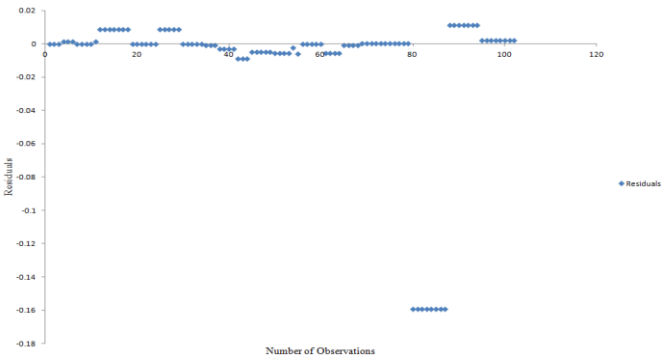

FIGURE 5.34 RESIDUAL PLOT OF TESTING DATA FOR θ_6

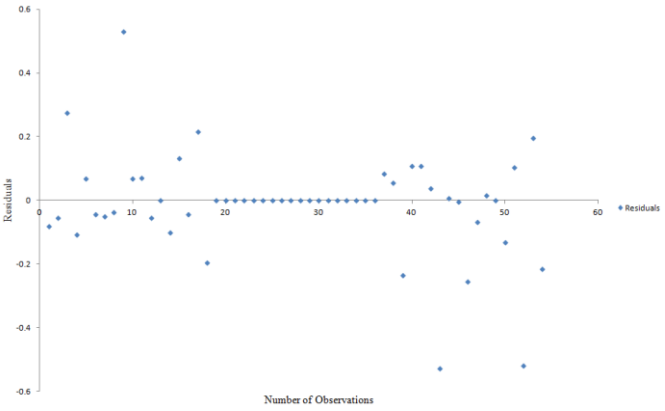

FIGURE 5.35 RESIDUAL PLOT OF TESTING DATA FOR θ_7

5.3 NORMAL PROBABILITY PLOT ANALYSIS

The normal probability plot is a graphical technique for assessing whether or not a data set is approximately normally distributed, if it is nearly straight, the data satisfy the nearly normal condition. The data are plotted against a theoretical normal distribution in such a way that the points should form an approximate straight line. Departures from this straight line indicate departures from normality. It provides a good assessment of the adequacy of the normal model for a set of data. It can also be defined as, in the normal probability plot; the normal distribution is represented by a straight line angled at 45 degrees. The actual distribution is plotted against this line so that any differences are shown as deviations from the straight line, making identification of differences quite apparent and interpretable. In this section, the normal probability

plot of residuals of training and testing data of all joint angles for the 5-DOF and 7-DOF Redundant manipulator is depicted in the following Figures. The Anderson-Darling test (AD Test) is also carried out to compare the fit of an observed cumulative distribution function to an expected cumulative distribution function. Smaller the AD value,
greater is the evidence that the data fit to the normal distribution. The following figures suggest that all the data are normally distributed. Similarly, the normal probability analysis is made for all training and testing data of all joint angles and signifies that the data are normally distributed.

5.3.1 Normal probability plot analysis of Training data for all joint angle of 5-DOF Redundant manipulator

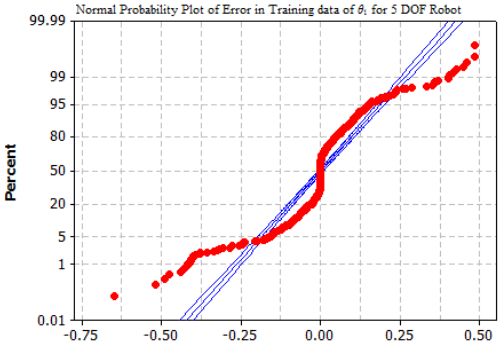

FIGURE 5.36 NORMAL PROBABILITY PLOT FOR RESIDUALS (TRAINING DATA OF)θ_1

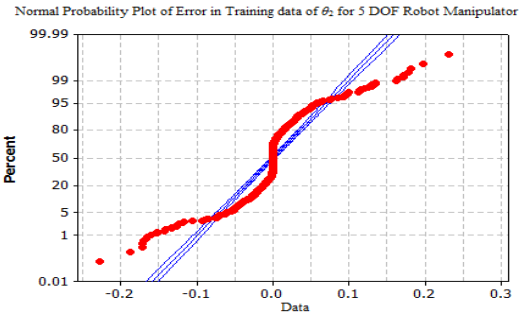

FIGURE 5.37 NORMAL PROBABILITY PLOT FOR RESIDUALS (TRAINING DATA OF θ_2)

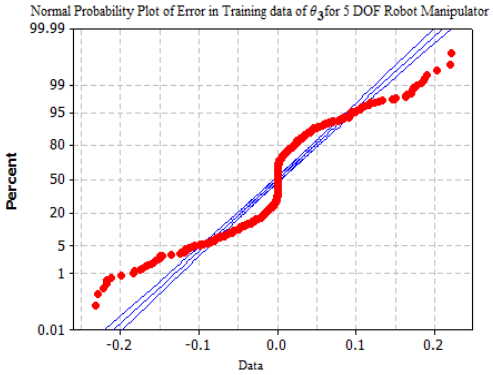

FIGURE 5.38 NORMAL PROBABILITY PLOT FOR RESIDUALS (TRAINING DATA OF) θ_3

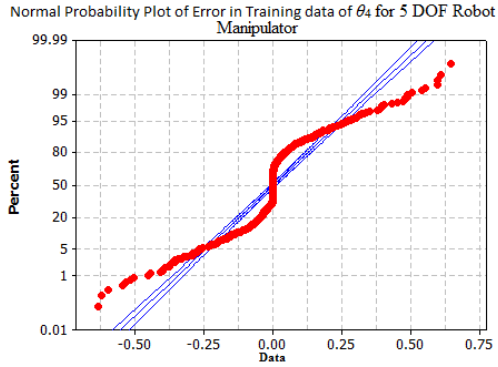

FIGURE 5.39 NORMAL PROBABILITY PLOT FOR RESIDUALS (TRAINING DATA OF)θ_4

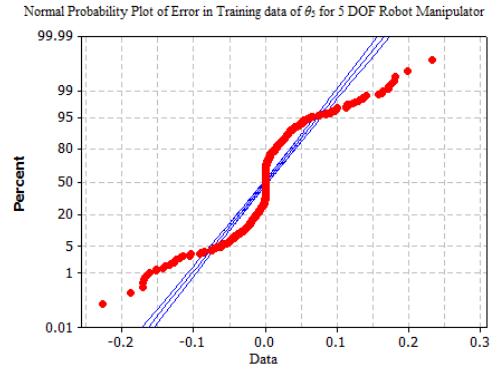

FIGURE 5.40 NORMAL PROBABILITY PLOT FOR RESIDUALS (TRAINING DATA OF)θ_5

5.3.2 Normal probability plot analysis of testing data for all joint angle of 5-DOF Redundant manipulator

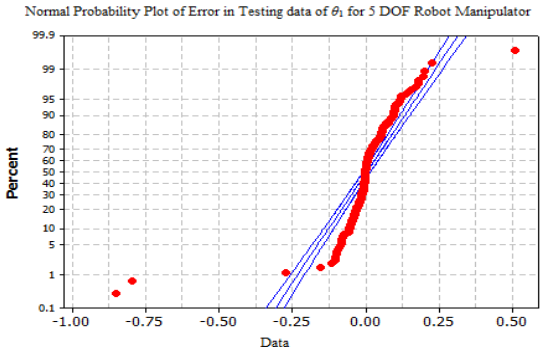

FIGURE 5.41 NORMAL PROBABILITY PLOT FOR RESIDUALS (TESTING DATA OF) θ_1

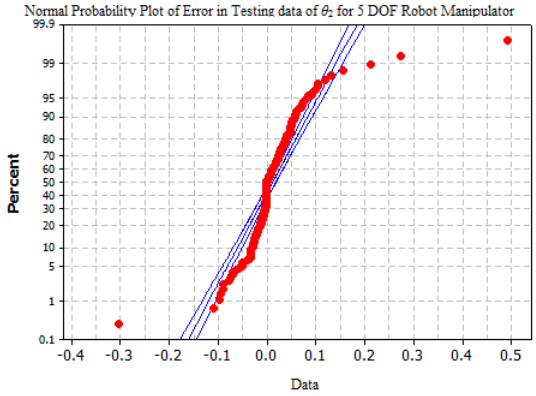

FIGURE 5.42 NORMAL PROBABILITY PLOT FOR RESIDUALS (TESTING DATA OF) θ_2

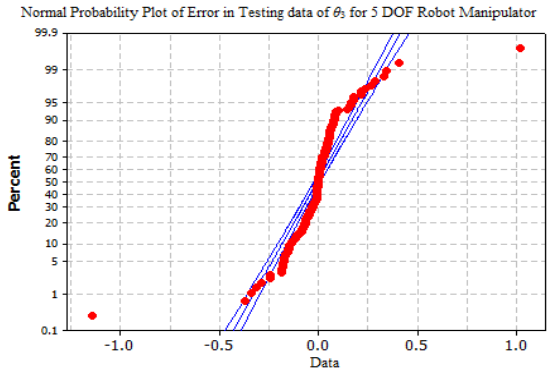

FIGURE 5.43 NORMAL PROBABILITY PLOT FOR RESIDUALS (TESTING DATA OF) θ_3

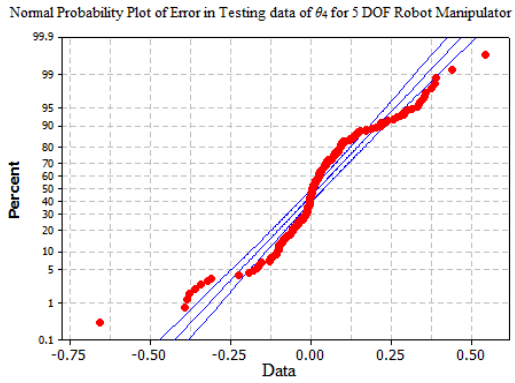

FIGURE 5.44 NORMAL PROBABILITY PLOT FOR RESIDUALS (TESTING DATA OF) θ_4

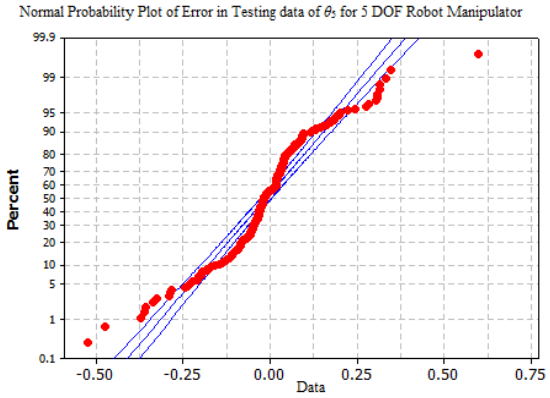

FIGURE5.45 NORMAL PROBABILITY PLOT FOR RESIDUALS (TESTING DATA OF) θ_5

5.3.3 Normal probability plot analysis of Training data for all joint angle of 7-DOF Redundant manipulator

The normal probability analysis of training and testing data for θ_3, $\theta_5$and θ_7 of 7-DOF Redundant manipulator is carried out in the following section similar to the 5-DOF Redundant manipulator. The data are plotted against a theoretical normal distribution in such a way that the points should form an approximate straight line. Departures from this straight line indicate departures from normality. It provides a good assessment of the adequacy of the normal model for a set of data. The Anderson-Darling test (AD Test) is also carried out similar to the 5-DOF Redundant manipulator, to compare the fit of an observed cumulative distribution function to an expected cumulative distribution function.

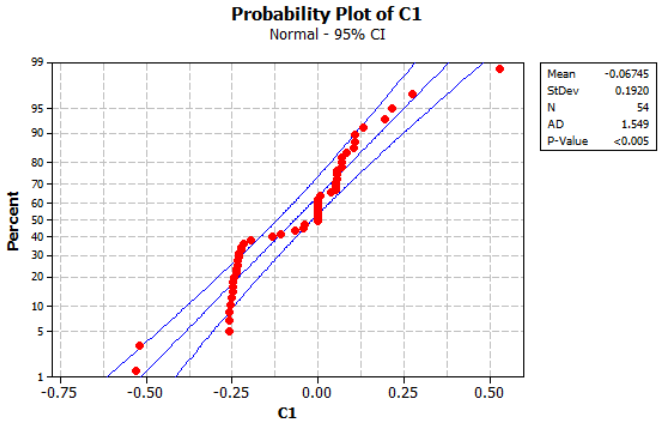

FIGURE5.46 NORMAL PROBABILITY PLOT FOR RESIDUALS (TRAINING DATA OF)θ_3

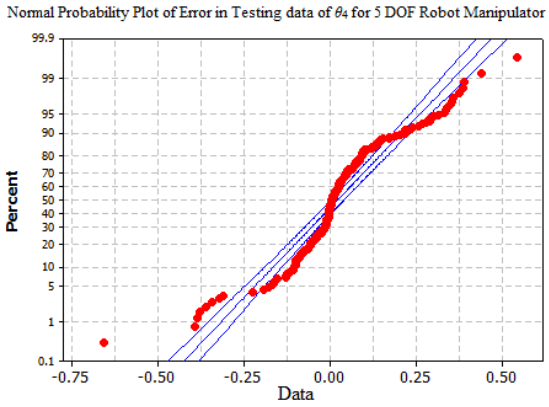

FIGURE 5.47 NORMAL PROBABILITY PLOT FOR RESIDUALS (TRAINING DATA OF) θ_5

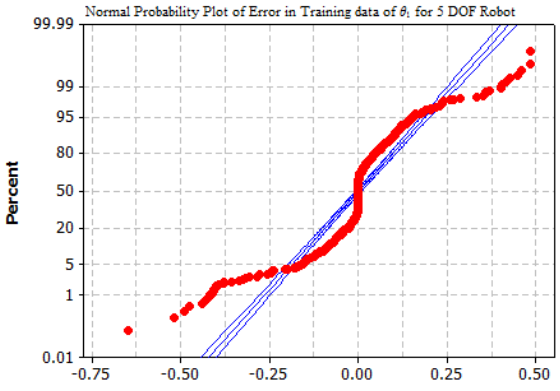

FIGURE 5.48 NORMAL PROBABILITY PLOT FOR RESIDUALS (TRAINING DATA OF) θ_7

5.3.4 Normal probability plot analysis of Testing data for all joint angle of 7-DOF Redundant manipulator

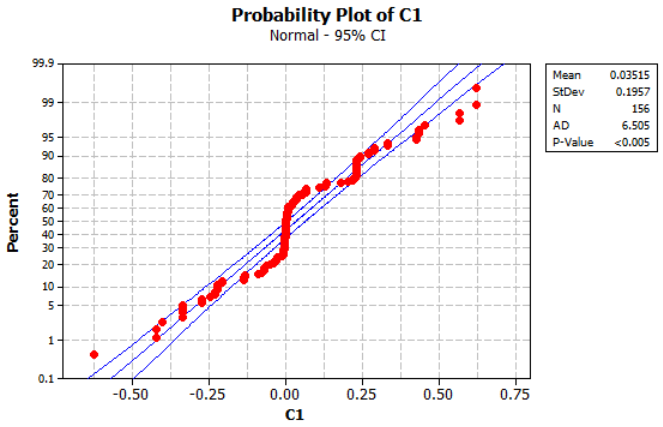

FIGURE 5.49 NORMAL PROBABILITY PLOT FOR RESIDUALS (TESTING DATA OF) θ_3

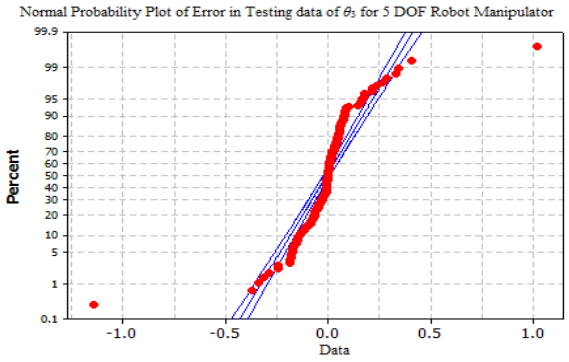

FIGURE 5.50 NORMAL PROBABILITY PLOT FOR RESIDUALS (TESTING DATA OF θ_5)

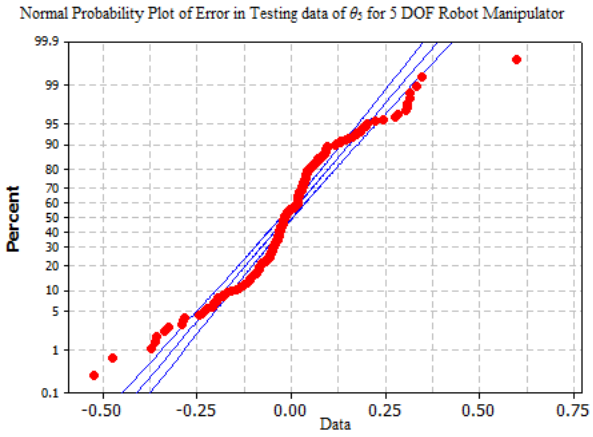

FIGURE 5.51 NORMAL PROBABILITY PLOT FOR RESIDUALS (TESTING DATA OF) θ_7

5.4 APPLICATION OF ARTIFICIAL NEURAL NETWORK (ANN)

In this work, an artificial neural network (ANN) model has also been adopted for estimating the IK

solution of a 7-DOF redundant manipulator. A comparative study of both the techniques i.e ANFIS and ANN has been carried out. In this work, for the construction of model, 3-30-7 feed forward ANN, input layer consisting of 3 nodes, single hidden layer containing 20 nodes with tangent sigmoid activation function, and the output layer containing 7 nodes with linear activation function is used. The architecture of the neural network used in the analysis is shownin the Figure.

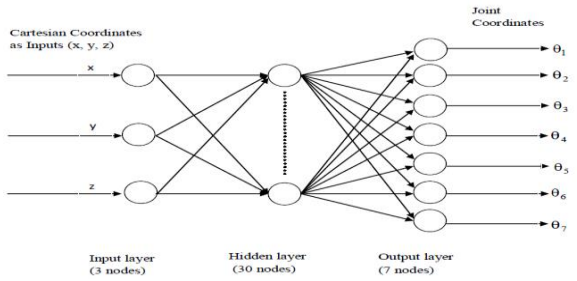

FIGURE 5.52 SCHEMATIC REPRESENTATION OF NEURAL NETWORK USED

In this analysis, MATLAB R2008a (Math Works, USA) software with its NN tool box is used for creating, training and testing the neural network. Here, 1638 data are taken as training and rest 549 data are taken as testing. The transfer function between input layer and hidden layer, hidden layer and output layer use tangent sigmoid function tansig() and linear function purelin() differently. Then, the learning rate (lr) is set to 0.07, MAX training steps epoch to 2000, show to 1000 and the Mean Square Error (MSE) of the network output as goal to 0.01. Then the network is trained with trainlm function of L-M algorithm. The key codes are listed as below:

net= newff ([-1 1; -1 1; -1 1],[30, 7], {'tansig', 'purelin', 'trainlm')};

net.trainparam.show= 1000;
net.trainparam.lr= 0.07;
net.trainparam.epochs= 2000;
net.trainparam.goal= 1e-3;
net= init(net);
net= train(net, pn, tn);

The performance of ANN and ANFIS model is compared using three statistics such as mean square error (MSE), mean bias error (MBE), and coefficient of determination (R^2).

$$MSE = \frac{\sum_{i=1}^{N}(P_i - A_i)^2}{N},$$

$$MBE = \frac{\sum_{i=1}^{N}(P_i - A_i)}{N},$$

$$R^2 = 1 - \frac{\sum_{i=1}^{N}(A_i - P_i)^2}{\sum_{i=1}^{N}(A_i - \tilde{A}_i)^2},$$

Where are the predicted, actual and average actual output of the network respectively and N is the total number of observation. The comparative analysis of training data (Tr) and testing data (Ts) of the ANFIS and ANN using three statistical criteria (MSE, MBE, R2) is being carried out and is tabulated in the following Table 5and Table 6. According to these tables, for ANN and ANFIS model, the MSE values range between 1.06 to 2.25 and between 0.046 to 0.623 respectively and R2 values range between 0.9150 to 0.9823 and 0.9448 to 0.9998 respectively. These are in narrow ranges. In all the analyses, the ANFIS model result in the better prediction of the inverse kinematics solution of the 7-DOF redundant manipulators. The ANFIS model outperformed the ANN model and provides the best performance i.e., lowest MSE, lowest MBE and highest R2. The results of the study also indicate that the predictive capability of ANN models used is poor as compared to the ANFIS model used for solving inverse kinematics equation of 7-DOF redundant manipulator. i i i A ~ and ,A , P

TABLE 5.1 PERFORMANCE OF ANFIS MODEL USED

	θ_1		θ_2		θ_3		θ_4		θ_5		θ_6		θ_7	
	Tr	Ts	Tr	Ts	Tr	Ts	Tr	Ts	Tr	Ts	Tr	Ts	Tr	Ts
MSE	0.124	0.133	0.042	0.058	0.373	0.125	0.447	0.623	0.337	0.529	0.128	0.201	0.231	0.248
MBE	0.008	0.015	0.004	0.030	0.033	0.125	0.036	0.061	0.030	0.037	0.022	0.044	0.041	0.067
R^2	0.9918	0.9842	0.9826	0.9760	0.9958	0.9448	0.9907	0.9889	0.9956	0.9497	0.9925	0.9689	0.9998	0.9484

TABLE 5.2 PERFORMANCE OF ANN MODEL USED

	θ_1		θ_2		θ_3		θ_4		θ_5		θ_6		θ_7	
	Tr	Ts	Tr	Ts	Tr	Ts	Tr	Ts	Tr	Ts	Tr	Ts	Tr	Ts
MSE	1.06	0.524	0.142	0.492	1.59	1.14	2.15	2.25	0.366	0.93	1.62	1.48	1.91	1.82
MBE	0.025	0.030	0.009	0.030	0.069	0.083	0.079	0.116	0.031	0.150	0.077	0.088	0.118	0.183
R^2	0.9647	0.9666	0.9719	0.9370	0.9765	0.9675	0.9370	0.9178	0.9520	0.9150	0.9712	0.9248	0.9703	0.9323

The MSE plot for training and testing data of all joint angles obtained from ANN and ANFIS are shown in

the Figure 5.52 respectively. It can be conclude from the Figures 5.21 and 5.22 that the MSE of training and testing data obtained from ANFIS model is reasonably low and meaningful error type as compare with the data obtained from ANN model. The MSE of the training data for joint angles θ_1 $\theta_2\theta_3\theta_6$ andθ_7 obtained from ANFIS model are acceptable and very low (0.124, 0.042, 0.373, 0.128, 0.231 respectively) as compare to ANN model which are very high (1.06, 0.142, 1.59, 1.62, 1.91 respectively). So the ANFIS model is more flexible than the model of ANN considered in this study for the prediction of inverse kinematics solution. This can be justified as the ANFIS approach provides a general frame work for the combination of neural networks and fuzzy logic. So the ANFIS models perform better than the ANN models in the prediction of inverse kinematic solution for 7-DOF redundant manipulator.

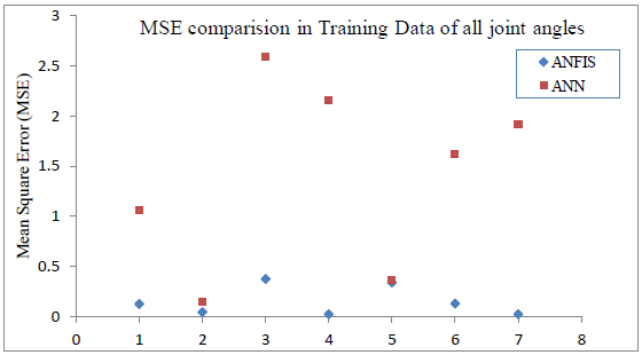

FIGURE 5.53 COMPARISON OF MEAN SQUARE ERROR PLOT FOR TRAINING DATA

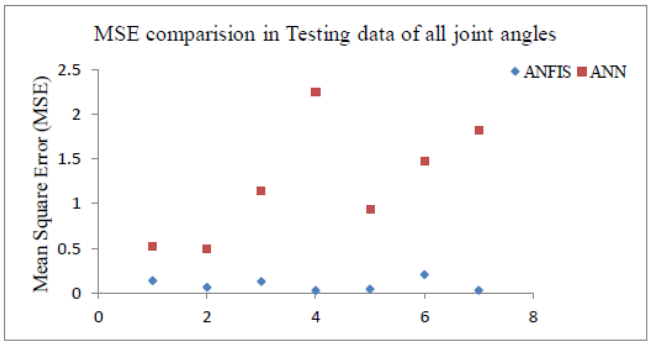

FIGURE 5.54 COMPARISON OF MEAN SQUARE ERROR PLOT FOR TESTING DATA.

By comparing the output from ANFIS and ANN model on the basis of global statistic i.e. MSE, MBE, and R2, it can be concludes that the ANFIS model is more flexible than the ANN model considered in this research, for prediction of IKs. As the ANFIS approach provides a general frame work for combination of NN and fuzzy logic. The efficiency of ANFIS over ANN can also be concluded by observing the graphs and tables which shows the comparison MSE, MBE, R2 for the two models. Based on comparison of the results of these two techniques, it is found that the proposed ANFIS model with Gaussian membership function is more efficient than the multilayer feed forward ANN using Levenberg-Marquardt (LM) algorithm for predicting the IK of the 7-DOF redundant manipulator.

VI. CONCLUSION

In this study, the inverse kinematics solution using ANFIS for a 5-DOF and 7-DOF Redundant manipulator is presented. The difference in joint angle deduced and predicted with ANFIS model for a 5-DOF and 7-DOF Redundant manipulator clearly depicts that the proposed method results with an acceptable error.Predicted (training data) values range from (-0.01 to 0.01) for both 5-DOF & 7- DOF and finding values (testing data) are range from (-0.03 to 0.03) it means the value decrease is about 0.02. The modelling efficiency of this technique was obtained by taking three end-effector coordinates as input parameters and five and seven joint positions for a 5-DOF and 7-DOF Redundant manipulator respectively as output parameters in training and testing data of NF models. Also, the ANFIS model used with a smaller number of iteration steps with the hybrid learning algorithm. Hence, the trained ANFIS model can be utilized to solve complex, nonlinear and discontinuous kinematics equation complex robot manipulator; thereby, making ANFIS an alternative approach to deal with inverse kinematics. The analytical inverse kinematics model derived always

provide correct joint angles for moving the arm end-effector to any given reachable positions and orientations.

As the ANFIS approach provides a general frame work for combination of NN and fuzzy logic. The efficiency of ANFIS for predicting the IK of Redundant manipulator can be concluded by observing the 3-D surface viewer, residual and normal probability graphs. The normal probability plots of the model are also plotted. The normal probability plot of residuals of training and testing data obtained from ANFIS shows that the data set of ANFIS are approximately normally distributed.

The methods used for deriving the inverse kinematics model for these manipulators could be applied to other types of robotic arms, such as the EduBots developed by the Robotica Ltd, Pioneer 2 robotic arm (P2Arm), 5-DOF Lynx 6 Educational Robot arm. It can be concluded that the solution developed in this paper will make the PArm more useful in application with unpredicted trajectory movement in unknown environment.

VII. SCOPE OF FUTURE WORK

In this work a hybrid neuro-fuzzy technology is used for the study of inverse kinematics of redundant robot manipulator. ANFIS is adopted for solving the IK of higher DOF robot manipulator. Due to its compactness and adaptive nature this technology is highly efficiency in predicting the IK of higher DOF robot manipulator. So this technology can use in different robot in different field to know the joint angles, orientations, and the robot working space to avoid obstacles.

VIII. REFERENCES

[1]. Deb S.R. Robotics technology and flexible automation, Tata McGrow-Hill Publishing Company Limited. New-Delhi, 2008.

[2]. Clarke, R. Asimov's Laws of Robotics: Implications for Information Technology- part II, Computer, 27(1), September (1994): pp.57–66.

[3]. Martin, F.G. Robotic Explorations: A Hands-On Introduction to Engineering, Prentice Hall, New Jersey, 2001.

[4]. Featherstone R. Position and velocity transformations between robot end-effector coordinates and joint angles. International journal of Robotic Research, SAGE Publications, 2(2), (1983), pp. 35-45.

[5]. Nieminen and Peetu, et al. Water hydraulic manipulator for fail safe and fault tolerant remote handling operations at ITER, Fusion Engineering and Design, Elsevier, Vol. 84, (2009), pp. 1420-1424.

[6]. Hollerbach J.M. Optimum kinematic design for seven degree of freedom manipulator, Second International Symposium on Robotics Research. Cambridge: MIT Press, (1985): pp. 215-222.

[7]. Sciavicco L. and Siciliano B. Modelling and Control of Robot Manipulators, Springer Second edition, (2000), Chapter 3, pp. 96.

[8]. Shimizu M., Kakuya H. Yoon W, Kitagaki K., and Kosuge K., Analytical Inverse Kinematic Computation for 7-DOF Redundant Manipulators with Joint Limits and its application to Redundancy. Resolution, IEEE Transaction on Robotics, October (2008), 24(5).

[9]. Vassilopoulos A.P and Bedi R. Adaptive neuro-fuzzy inference system in modelling fatigue life of multidirectional composite laminates, Computation and Material Science.43 (2008): pp. 1086-1093.

[10]. Haykin S., Neural Networks- A Comprehensive Foundation, McMillan College Publishing, New York, 1998.

[11]. Mendel J.M. Fuzzy logic system for engineering: A tutorial, Proceeding, IEEE. 83(3) (1995): pp. 345-377.

[12]. Ke L., Hong-ge M., Hai-jing Z. Application of Adaptive Neuro-Fuzzy Inference System to Forecast of Microwave Effect, IEEE Conference Publications, (2009) , pp. 1- 3.

[13]. Alavandar S. and Nigam M. J. Adaptive Neuro-Fuzzy Inference System based control of six DOF robot manipulator, Journal of Engineering Science and Technology Review,1 (2008): pp.106- 111.

[14]. Craig J.J. Introduction to Robotics: Mechanisms and Controls, Addison-Wesley, Reading, MA, 1989.

[15]. Lee G.C.S. Dynamics and Control, Robot Arm Kinematics, Computer, 15(1982), Issue.12: pp. 62-79.

[16]. Korein J.U and Balder N.I. Techniques for generating the goal-directed motion of articulated structures', Institute of Electrical and Electronics Engineers Computer Graphics Applications, 2(1982), Issue. 9: pp. 71-81.

[17]. Srinivasan A and Nigam M.J. 'Neuro-Fuzzy based Approach for Inverse Kinematics Solution of Industrial Robot Manipulators', International Journal of Computers, Communications and Control, III (2008), No. 3: pp. 224-234.

[18]. Calderon C.A.A., Alfaro E.M.R.P, Gan J.Q. and Hu H. Trajectory generation and tracking of a 5-DOF Robotic Arm. CONTROL, University of Bath, (2004).

[19]. De X., Calderon C.A.A., Gan J.Q., H Hu. An Analysis of the Inverse Kinematics for a 5-DOF Manipulator, International Journal of Automation and Computing, (2) (2005): pp. 114-124.

[20]. Gan J.Q., Oyama E., Rosales E.M. and Hu, H. A complete analytical solution to the inverse kinematics of the Pioneer 2 robotic arm, Robotica, Cambridge University Press. 23(2005): pp. 123–129.

[21]. Hasan A.T. and Al-Assadi H.M.A.A. Performance Prediction Network for Serial Manipulators Inverse Kinematics Solution Passing Through Singular Configurations, International Journal of Advanced Robotic Systems, 7(2010), No. 4: pp. 10-23.

Cite this article as :

Mohit Kumar, B. S. Choudhary, "Inverse Kinematic Analysis of 5-DOF and 7-DOF Redundant Manipulator using ANFIS ", International Journal of Scientific Research in Computer Science, Engineering and Information Technology (IJSRCSEIT), ISSN : 2456-3307, Volume 9, Issue 2, pp.97-127, March-April-2023.